

## Discovery of Clinical Candidate 1-[(2S,3S,4S)-3-Ethyl-4-fluoro-5-oxopyrrolidin-2-yl]methoxy}-7-methoxyisoquinoline-6-carboxamide (PF-06650833), a Potent, Selective Inhibitor of Interleukin-1 Receptor Associated Kinase 4 (IRAK4), by Fragment-Based Drug Design

Katherine L. Lee,<sup>\*†‡</sup> Catherine M. Ambler,<sup>#</sup> David R. Anderson,<sup>▽¶</sup> Brian P. Boscoe,<sup>||</sup> Andrea G. Bree,<sup>‡</sup> Joanne I. Brodfuehrer,<sup>§</sup> Jeanne S. Chang,<sup>||</sup> Chulho Choi,<sup>||</sup> Seungwon Chung,<sup>||,†</sup> Kevin J. Curran,<sup>†,●</sup> Jacqueline E. Day,<sup>▽,△</sup> Christoph M. Dehnhardt,<sup>†,□</sup> Ken Dower,<sup>‡</sup> Susan E. Drozda,<sup>||</sup> Richard K. Frisbie,<sup>†</sup> Lori K. Gavrin,<sup>†,▲</sup> Joel A. Goldberg,<sup>†,◎</sup> Seungil Han,<sup>||</sup> Martin Hegen,<sup>‡</sup> David Hepworth,<sup>†</sup> Heidi R. Hope,<sup>○,■</sup> Satwik Kamtekar,<sup>▽</sup> Iain C. Kilty,<sup>‡</sup> Arthur Lee,<sup>†</sup> Lih-Ling Lin,<sup>‡</sup> Frank E. Lovering,<sup>†,○</sup> Michael D. Lowe,<sup>†,▼</sup> John P. Mathias,<sup>†</sup> Heidi M. Morgan,<sup>◆,★</sup> Elizabeth A. Murphy,<sup>‡</sup> Nikolaos Papaioannou,<sup>†,▲</sup> Akshay Patny,<sup>†,△</sup> Betsy S. Pierce,<sup>▽,●</sup> Vikram R. Rao,<sup>‡</sup> Eddine Saiah,<sup>†,☆</sup> Ivan J. Samardjiev,<sup>||</sup> Brian M. Samas,<sup>||</sup> Marina W. H. Shen,<sup>‡</sup> Julia H. Shin,<sup>‡</sup> Holly H. Soutter,<sup>||,○</sup> Joseph W. Strohbach,<sup>†</sup> Peter T. Symanowicz,<sup>‡</sup> Jennifer R. Thomason,<sup>†,§</sup> John D. Trzupek,<sup>†,◆</sup> Richard Vargas,<sup>†,▶</sup> Fabien Vincent,<sup>†</sup> Jiangli Yan,<sup>◆</sup> Christoph W. Zapf,<sup>†,△</sup> and Stephen W. Wright<sup>\*,||</sup>

<sup>†</sup>Medicine Design, <sup>‡</sup>Inflammation and Immunology Research Unit, and <sup>§</sup>Medicine Design, Pfizer Inc., 1 Portland Street, Cambridge, Massachusetts 02139, United States

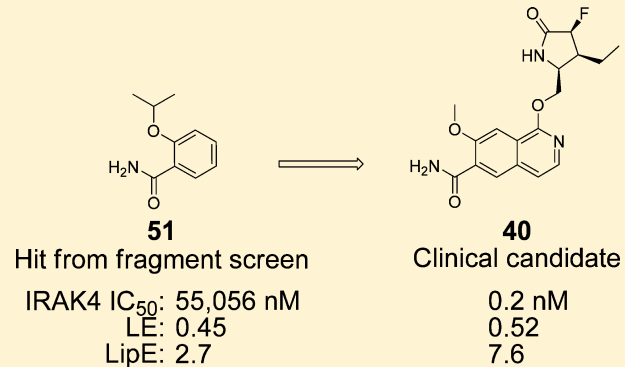
<sup>||</sup>Medicine Design, <sup>▽</sup>Medicine Design, <sup>#</sup>Medicinal Sciences, Pfizer Inc., 445 Eastern Point Road, Groton, Connecticut 06340, United States

<sup>▽</sup>Worldwide Medicinal Chemistry and <sup>○</sup>Inflammation and Immunology Research Unit, Pfizer Inc., 700 Chesterfield Parkway West, St. Louis, Missouri 63017, United States

<sup>◆</sup>Worldwide Medicinal Chemistry, Pfizer Inc., 1070 Science Center Drive, San Diego, California 92121, United States

### Supporting Information

**ABSTRACT:** Through fragment-based drug design focused on engaging the active site of IRAK4 and leveraging three-dimensional topology in a ligand-efficient manner, a micromolar hit identified from a screen of a Pfizer fragment library was optimized to afford IRAK4 inhibitors with nanomolar potency in cellular assays. The medicinal chemistry effort featured the judicious placement of lipophilicity, informed by co-crystal structures with IRAK4 and optimization of ADME properties to deliver clinical candidate PF-06650833 (compound **40**). This compound displays a 5-unit increase in lipophilic efficiency from the fragment hit, excellent kinase selectivity, and pharmacokinetic properties suitable for oral administration.



### INTRODUCTION

Interleukin-1 receptor associated kinase 4 (IRAK4) is a key node in innate inflammatory signaling directly downstream of the Toll-like receptors (TLRs) and interleukin-1 (IL-1) family of receptors.<sup>1</sup> TLRs represent a first line of defense against pathogens such as bacteria, viruses, and yeast. The IL-1 family of receptors also plays important roles in the immediate inflammatory response to invading organisms. In addition, IRAK4 is expressed in T and B lymphocytes and has been reported to play an important role in cross talk between the innate and adaptive immune systems.<sup>1–5</sup> IRAK4 has both a

kinase dependent signaling role as well as a scaffolding role in a larger signaling complex including proteins such as myeloid differentiation primary response gene 88 (MYD88) and IRAK1.<sup>6,7</sup> Interestingly, individuals who lack IRAK4 show impaired activation of the innate immune response but no increased susceptibility to viral or fungal infection and only increased infection risk by a narrow range of pyogenic bacteria prior to adolescence.<sup>8,9</sup> This suggests that selective small

Received: February 10, 2017

Published: May 12, 2017



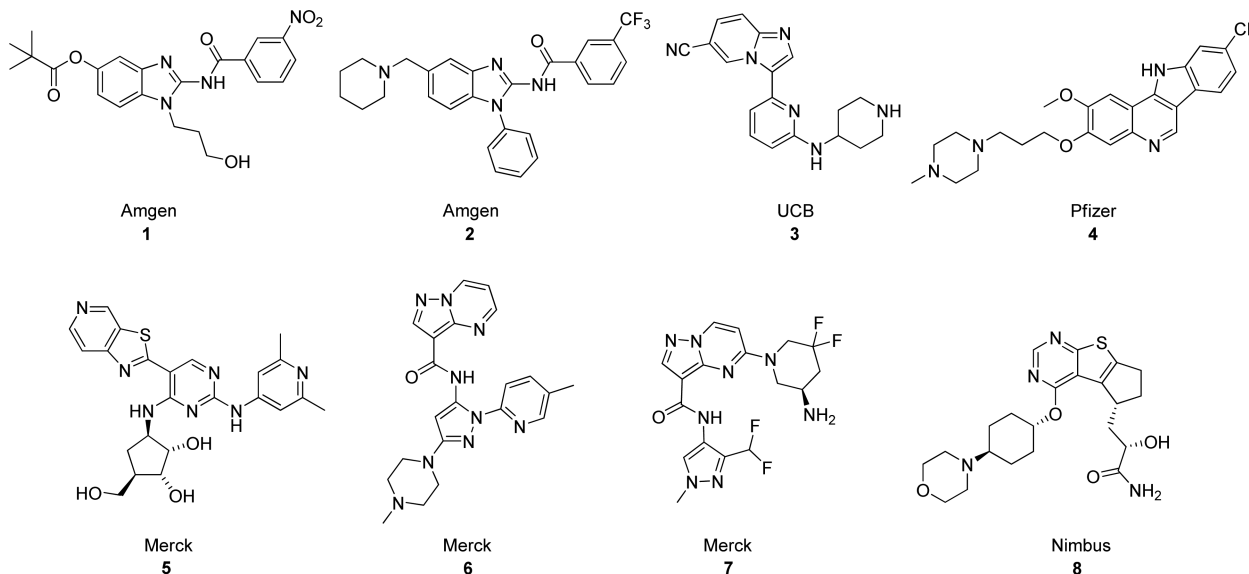


**Figure 1.** Representative IRAK4 inhibitors from the peer-reviewed literature.

small molecule inhibitors of IRAK4 may have anti-inflammatory activity, attenuating the innate immune response while avoiding broad immunosuppression.

Aberrant activation of the innate immune system is characteristic of a number of chronic autoimmune diseases. For example, both the anticitrullinated antibody immune complexes characteristic of active rheumatoid arthritis (RA) and the antinucleic acid immune complexes characteristic of systemic lupus erythematosus (SLE) signal through TLRs.<sup>10,11</sup> Moreover, activation of TLRs can prime differentiation of B cells to antibody producing plasma cells, thus serving to prime the adaptive immune system.<sup>12</sup> Genetically modified mice either having IRAK4 deletion or expressing a kinase-inactive form of IRAK4 have an impaired immune response to TLR stimulation such as bacterial lipopolysaccharide (LPS) induced TNF $\alpha$  and IL-6 induction.<sup>13</sup> These mice are also resistant to experimentally induced arthritis,<sup>14</sup> atherosclerosis,<sup>15</sup> and MOG-induced encephalomyelitis.<sup>16</sup> IRAK4 kinase-inactive mice have also been shown to be resistant to the development of Alzheimer's disease, a process that is thought to be due to reduced IL-1 production and signaling.<sup>17</sup> Similarly, small molecule inhibitors of IRAK4 have been reported to inhibit TLR induced inflammatory signaling in vitro and in vivo.<sup>18,19</sup> In addition, in vivo administration of IRAK4 inhibitors has been observed to reduce gout-like inflammation in the uric acid induced peritonitis model,<sup>19</sup> ischemia induced inflammation in 5/6 nephrectomized rats,<sup>20</sup> and mouse models of lupus.<sup>21</sup> IRAK4 has therefore been recognized as an important pharmacological target for the treatment of chronic inflammatory diseases.

Supported by this strong rationale, and as evidenced by numerous reports in the peer-reviewed and patent literature, there have been significant efforts at many companies to identify potent, selective, and safe IRAK4 inhibitors suitable for clinical study. Indeed, in the past decade, small molecule IRAK4 inhibitors of various chemotypes have been described in the literature. A selection of examples is shown in Figure 1, including aminobenzimidazoles,<sup>22–24</sup> imidazopyridines,<sup>25,26</sup> indoloquinolines,<sup>18</sup> diaminopyridines,<sup>27</sup> amidopyrazoles,<sup>28,29</sup> and thienopyrimidines.<sup>19</sup> The literature and patent landscapes have been extensively reviewed,<sup>30–33</sup> further demonstrating the breadth of effort expended on IRAK4. Despite this substantial investment,

there are few reports of IRAK4 inhibitors reaching clinical study. Herein we describe the discovery of an IRAK4 inhibitor clinical candidate resulting from fragment-based drug design.

The active site of IRAK4 has a number of features that make this a challenging kinase target for drug discovery. IRAK4 has a tyrosine gatekeeper residue (Tyr262 in IRAK4); tyrosine gatekeeper residues are unique to the IRAK family. Tyr262, Lys213, and Asp329 collectively block access to the deep pocket commonly accessed by inhibitors of other kinases and define a relatively small ATP site. This suggests that unconventional strategies might be needed to achieve selectivity for IRAK4 versus other kinases (Figure 2).

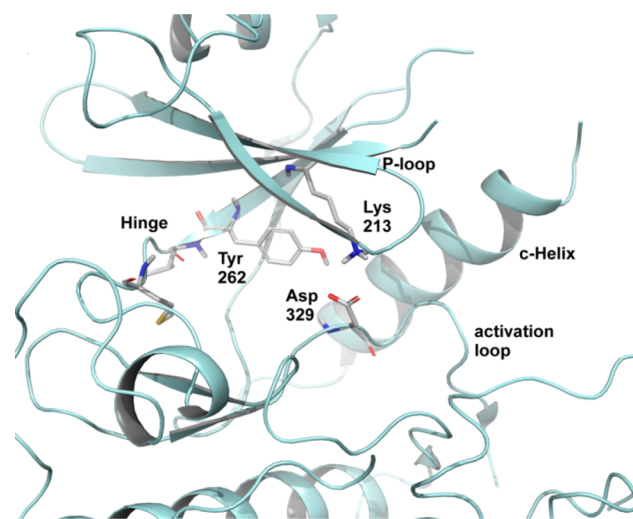


**Figure 2.** Crystal structure of IRAK4 active site highlighting the back of the binding site as defined by gatekeeper Tyr262 and Lys213.

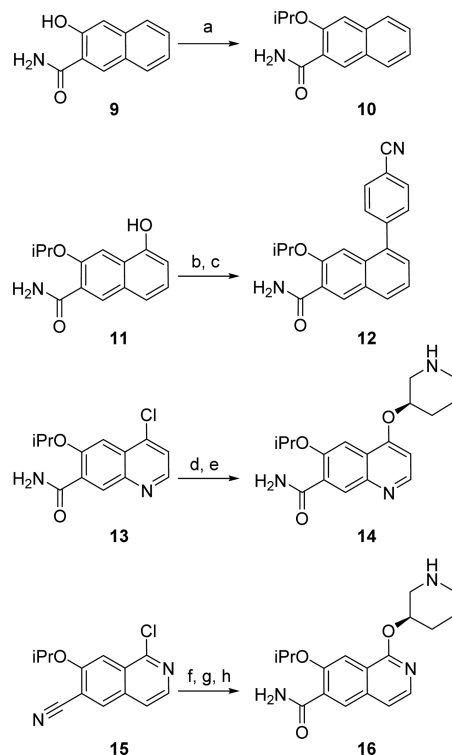
As noted, several earlier reports of efforts to discover inhibitors of IRAK4 led to inhibitors with flat binding topologies, with a high fraction of  $sp^2$  atoms and bearing commonly used kinase hinge-binding motifs. This includes Pfizer's previously reported fused tetracycles exemplified by 4.<sup>18</sup> We reasoned that, to get the high potency and kinase selectivity required to deliver a safe and effective inhibitor, we would benefit from fully exploiting the

three-dimensional shape of the ATP-binding site. On the basis of the first IRAK4 inhibitor co-crystal structure (2NRU),<sup>22</sup> it has been proposed<sup>30</sup> that IRAK4 possesses a unique “front pocket” that may offer opportunities to achieve selective IRAK4 inhibition. Recently, additional protein–ligand structures have been published<sup>28,29</sup> which utilize this same front pocket as well as occupying the ribose binding region of the ATP pocket. To maximize our chances of finding inhibitors that fully utilized the available binding opportunities in the IRAK4 ATP site, we elected to adopt a fragment-based lead seeking approach.<sup>34</sup>

## ■ SYNTHESIS OF POTENTIAL INHIBITORS

Analogues 10, 12, 14, and 16 in Table 1 were prepared as shown in Scheme 1. The syntheses of the naphthalene (9 and 11),

**Scheme 1. Synthesis of Analogues 10, 12, 14, and 16<sup>a</sup>**



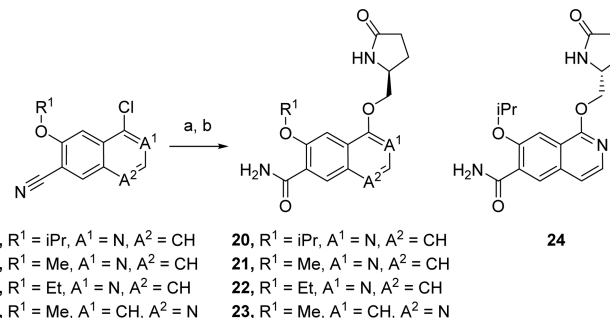
<sup>a</sup>Conditions: (a)  $(\text{CH}_3)_2\text{CHI}$ ,  $\text{K}_2\text{CO}_3$ , DMSO,  $130^\circ\text{C}$ , 2 h, 92%; (b)  $\text{NaH}$ ,  $\text{PhNTF}_2$ , THF,  $20^\circ\text{C}$ , 1 h; (c)  $\text{NCC}_6\text{H}_4\text{B}(\text{OH})_2$ ,  $\text{Pd}(\text{PPh}_3)_4$ ,  $\text{Na}_2\text{CO}_3$ ,  $\text{H}_2\text{O}$ , PhMe, EtOH, reflux, 2 h, 72% (2 steps); (d) *tert*-butyl (*R*)-3-hydroxypiperidine-1-carboxylate,  $\text{KOtBu}$ , DMSO,  $60^\circ\text{C}$ , 3 h; (e) TFA, DCM,  $20^\circ\text{C}$ , 4 h, 94% (2 steps); (f) *tert*-butyl (*R*)-3-hydroxypiperidine-1-carboxylate, KHMDS, DMF,  $-10^\circ\text{C}$ , 3 h; (g)  $\text{K}_2\text{CO}_3$ ,  $\text{H}_2\text{O}_2$ , DMSO,  $20^\circ\text{C}$ , 2 h; (h) 4 M HCl, dioxane,  $20^\circ\text{C}$ , 1 h, 65% (3 steps).

quinoline (13), and isoquinoline (15) starting materials were guided by established procedures for the preparation of similar compounds,<sup>35,36</sup> and the syntheses of compounds 11, 13, and 15 have been described.<sup>37</sup> Alkylation of naphthol 9 afforded the naphthyl ether 10. Naphthol 11 was transformed to 12 by Suzuki coupling of an intermediate naphthyl triflate with (4-cyano)-phenylboronic acid. Compounds 14 and 16 were prepared by  $\text{S}_{\text{N}}\text{Ar}$  reactions of the chloroquinoline 13 and the chloroisoquinoline 15, respectively, with *tert*-butyl (*R*)-3-hydroxypiperidine-1-carboxylate followed by deprotection; in the case of the isoquinoline 15, a nitrile hydration step was required, which was

readily accomplished by the use of  $\text{K}_2\text{CO}_3$  and 30% hydrogen peroxide in DMSO solution at  $20^\circ\text{C}$ .

The target compounds in Tables 2 and 3 were prepared by coupling of the bicyclic aromatic cores with appropriately substituted alcohol fragments, as shown in the accompanying schemes. The key bond connections were made by  $\text{S}_{\text{N}}\text{Ar}$  reactions in the case of quinolines and isoquinolines (Scheme 2)

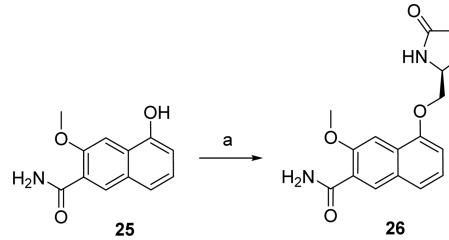
**Scheme 2. Preparation of Analogs 20–24<sup>a,b</sup>**



<sup>a</sup>Conditions: (a) (S)-5-(hydroxymethyl)pyrrolidin-2-one, KHMDS, DMF,  $-10^\circ\text{C}$ , 3 h, 51–97%; (b)  $\text{K}_2\text{CO}_3$ ,  $\text{H}_2\text{O}_2$ , DMSO,  $20^\circ\text{C}$ , 2 h, 47–98%. <sup>b</sup>Compound 24 was prepared from 15 and (R)-5-(hydroxymethyl)pyrrolidinone in an analogous fashion to the preparation of compound 20.

and by Mitsunobu reactions in the case of naphthalenes (Scheme 3). The bicyclic aromatic starting materials 17–19 and 25 were

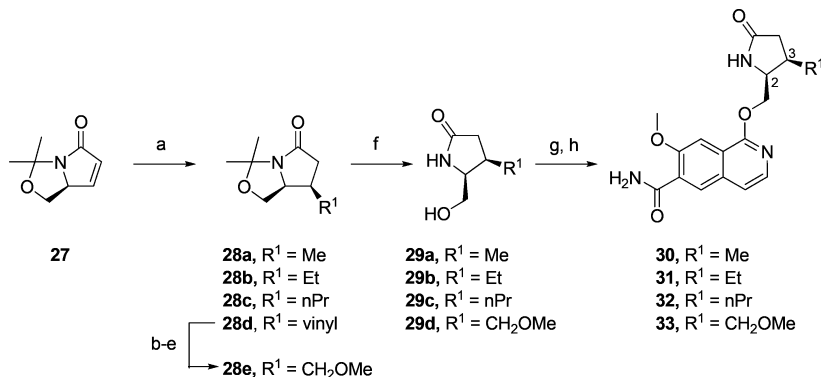
**Scheme 3. Preparation of Analogue 26<sup>a</sup>**



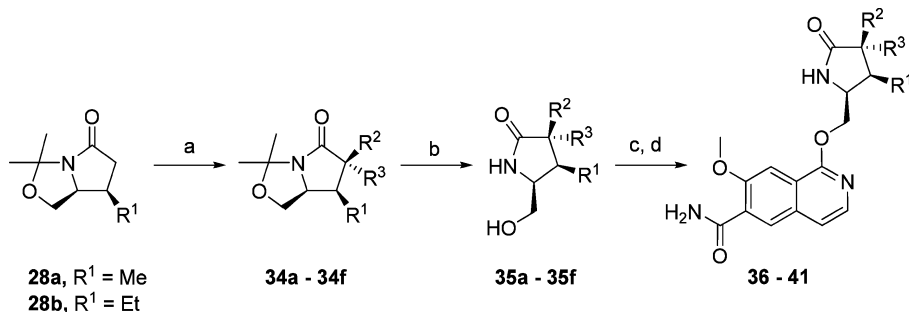
<sup>a</sup>Conditions: (a) (S)-5-(hydroxymethyl)pyrrolidin-2-one,  $\text{PPh}_3$ , DEAD, THF,  $70^\circ\text{C}$ , 24 h, 45%.

prepared by procedures similar to those used previously for the preparation of 11, 13, and 15, and the syntheses of 17–19 and 25 have likewise been described.<sup>37</sup> The  $\text{S}_{\text{N}}\text{Ar}$  reactions were found to proceed best using a homogeneous potassium base such as potassium bis(trimethylsilyl)amide in a minimum volume of dipolar aprotic solvent at temperatures of  $-10$  to  $0^\circ\text{C}$ . In most cases, the  $\text{S}_{\text{N}}\text{Ar}$  reactions were followed by nitrile hydration to the primary amide as the last step. These were accomplished using  $\text{H}_2\text{O}_2$  and  $\text{K}_2\text{CO}_3$  as previously noted.

Our attention soon focused upon alcohol fragments derived from (S)-5-(hydroxymethyl)pyrrolidin-2-one, as shown in Table 2. Further elaboration of these alcohol fragments afforded targets shown in Table 3. Intermediates 28a–28d (Scheme 4) were prepared as previously described<sup>38</sup> by a *syn*-selective conjugate addition reaction to  $\alpha,\beta$ -unsaturated lactam 27<sup>38</sup> that afforded the acetonide-protected bicyclic lactams as single diastereomers. The vinyl bicyclic lactam 28d<sup>38</sup> was converted to the 3(*R*)-methyl ether 28e by functional group manipulation involving oxidative cleavage to an aldehyde and reduction to the alcohol, followed by alkylation to provide the methyl ether. Cleavage of

Scheme 4. Preparation of Analogs 30–33<sup>a</sup>

<sup>a</sup>Conditions: (a) RM, Cu(I), TMSCl, THF, 39–82%; (b) O<sub>3</sub>, DCM, MeOH, −78 °C, 2 h; (c) Me<sub>2</sub>S, −78 °C, 30 min; (d) NaBH<sub>4</sub>, −78 to 20 °C, 2 h; (e) Ag<sub>2</sub>O, MeI, THF, 70 °C, 16 h, 44% (4 steps); (f) TsOH (0.1 equiv), MeCN, H<sub>2</sub>O, 90 °C, 2 h; (g) 17, KHMDS, DMF, −10 °C, 3 h; (h) K<sub>2</sub>CO<sub>3</sub>, H<sub>2</sub>O<sub>2</sub>, DMSO, 20 °C, 2 h.

Scheme 5. Preparation of Analogs 36–41<sup>a</sup>

Starting Material	Electrophile	R <sup>1</sup>	R <sup>2</sup>	R <sup>3</sup>	Diastereomer	Acetonide	Alcohol	Target
<b>28a</b>	MeI	Me	Me	H	<i>syn</i>	<b>34a</b>	<b>35a</b>	<b>36</b>
<b>28a</b>	MeI	Me	H	Me	<i>anti</i>	<b>34b</b>	<b>35b</b>	<b>37</b>
<b>28a</b>	NFSI	Me	F	H	<i>syn</i>	<b>34c</b>	<b>35c</b>	<b>38</b>
<b>28a</b>	NFSI	Me	H	F	<i>anti</i>	<b>34d</b>	<b>35d</b>	<b>39</b>
<b>28b</b>	NFSI	Et	F	H	<i>syn</i>	<b>34e</b>	<b>35e</b>	<b>40</b>
<b>28b</b>	NFSI	Et	H	F	<i>anti</i>	<b>34f</b>	<b>35f</b>	<b>41</b>

<sup>a</sup>Conditions: (a) LDA, THF, −78 °C, 30 min, then electrophile, −78 to 20 °C, 2 h; (b) TsOH (0.1 equiv), MeCN, H<sub>2</sub>O, 90 °C, 2 h; (c) 17, KHMDS, DMF, −10 °C, 3 h; (d) K<sub>2</sub>CO<sub>3</sub>, H<sub>2</sub>O<sub>2</sub>, DMSO, 20 °C, 2 h.

the acetonide groups with catalytic acid in the presence of water afforded the appropriately substituted lactam alcohols 29a–29e, which were then subjected to S<sub>N</sub>Ar reactions and nitrile hydrations to afford analogues 30–33.

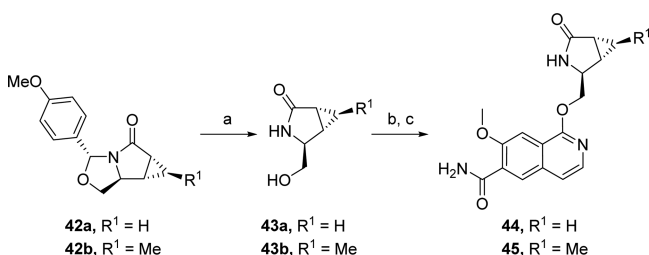
The synthesis of substituted lactam analogues 36–41 was accomplished as shown in Scheme 5, similarly to procedures described for the fluorination<sup>39,40</sup> and alkylation<sup>41</sup> of the unsubstituted bicyclic lactam. Enolate generation was accomplished by treatment of compounds 28a–28b with LDA in THF at −78 °C. Subsequent trapping with CH<sub>3</sub>I or N-fluorobis(phenylsulfonyl)imide (NFSI) afforded the substituted bicyclic lactams 34a–34f as separable mixtures of diastereomers. In each

case, the major diastereomer resulted from substitution of the enolate *anti* to the previously placed substituents, as would be expected from steric considerations.<sup>42</sup> Stereochemical assignments were made by NOE experiments, and the heteronuclear <sup>19</sup>F–<sup>1</sup>H NOE results were confirmed by single-crystal X-ray structure determination of the bicyclic lactam 34e (see Supporting Information). In the case of the fluoro-substituted lactams 34c–34f, the individual diastereomers could be epimerized by exposure to a base such as powdered KOH. However, once the acetonide protecting group had been cleaved, the resulting fluoro-substituted lactam alcohols 35c–35f proved to be remarkably resistant to epimerization by base, for example,

during the subsequent  $S_NAr$  reaction. Presumably, this was a result of initial deprotonation of the lactam NH and the consequent difficulty of generating an enolate adjacent to the lactam anion.

The cyclopropane targets in **Table 3** were prepared as shown in **Scheme 6** from the (4-methoxy)-benzylidene precursors **42a**

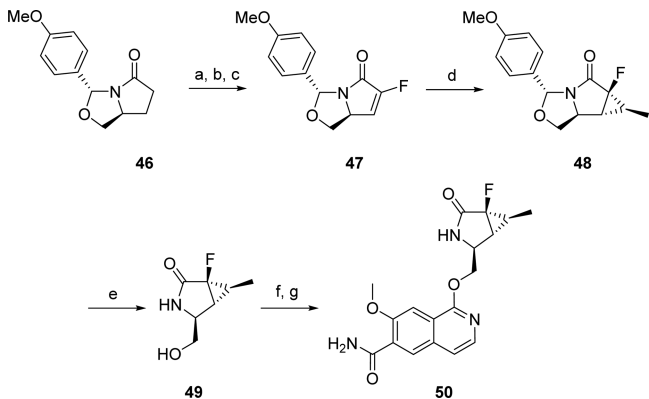
**Scheme 6. Preparation of 44 and 45<sup>a</sup>**



<sup>a</sup>Conditions: (a) TsOH (0.1 equiv), MeCN, H<sub>2</sub>O, 90 °C, 2 h; (b) 17, KHMDS, DMF, -10 °C, 3 h; (c) K<sub>2</sub>CO<sub>3</sub>, H<sub>2</sub>O<sub>2</sub>, DMSO, 20 °C, 2 h.

and **42b**, which were in turn prepared using a stereoselective cyclopropanation reaction.<sup>43,44</sup> A single-crystal X-ray structure of intermediate **42b** established the stereochemistry of cyclopropane target **45**. The fluorinated cyclopropane **50** was prepared by a similar cyclopropanation approach from the fluoro-olefin **47** as shown in **Scheme 7**. The fluoro-olefin **47** was

**Scheme 7. Preparation of 50<sup>a</sup>**



<sup>a</sup>Conditions: (a) LDA, THF, -78 °C, 30 min, then NFSI, -78 to 20 °C, 90 min; (b) LDA, THF, -78 °C, 30 min, then PhSeSePh, -78 to 20 °C, 90 min; (c) H<sub>2</sub>O<sub>2</sub>, pyr, DCM, 20 °C, 3 h, 25% (3 steps); (d) LDA, Ph<sub>2</sub>SEtBF<sub>4</sub>, DME, -45 °C, 45 min, then 47, -30 °C, 90 min, 16%; (e) TsOH (0.1 equiv), MeCN, H<sub>2</sub>O, 90 °C, 2 h; (f) 17, KHMDS, DMF, -10 °C, 3 h; (g) K<sub>2</sub>CO<sub>3</sub>, H<sub>2</sub>O<sub>2</sub>, DMSO, 20 °C, 2 h.

prepared from **46** by fluorination, followed by a two-step sequence of selenenylation and oxidation.<sup>45</sup> The stereochemical assignment of **50** was derived from the single-crystal X-ray structure determination of the bicyclic lactam **48** (see the Supporting Information).

## ■ IN VITRO ASSAYS

IRAK4 enzyme potency was measured in a DELFIA assay using activated full-length IRAK4 protein in the presence of 600 μM ATP (i.e., ATP  $K_m$ ) and assessing phosphorylation of a peptide substrate. IRAK4 cell potency was assessed by measuring R848-stimulated TNF $\alpha$  production in peripheral blood mononuclear cells (PBMCs) isolated from human blood. A whole blood assay

of R848-stimulated IL-6 production in human whole blood was also employed. Potency in the human whole blood assay, when corrected for plasma protein binding by multiplying the IC<sub>50</sub> by the fraction unbound as measured by equilibrium dialysis, was largely in agreement with the potency determined in the cellular assay in PBMCs.

## ■ RESULTS AND DISCUSSION

The Pfizer Global Fragment Initiative library<sup>46</sup> of 2592 fragment compounds was screened against the kinase domain of IRAK4 using a NMR saturation transfer difference (STD) assay at a compound concentration of 236 μM and IRAK4 concentration of 3 μM to identify 169 fragment hits for which >10% STD was observed. Concurrently, the same fragment collection was submitted to an IRAK4 Caliper assay to identify 160 fragment hits with >50% inhibition at 909 μM. Next, 160 fragment hits, including 95 fragments identified as hits in both the NMR STD and biochemical assays, were characterized by an NMR ATP-functional assay measuring the conversion of ATP to ADP. From this effort, coupled with modeling to identify potential hinge-binding fragments, 15 fragment hits were prioritized and advanced to cocrystallization experiments, leading to 10 crystal structures with IRAK4 kinase domain (Figure 3).

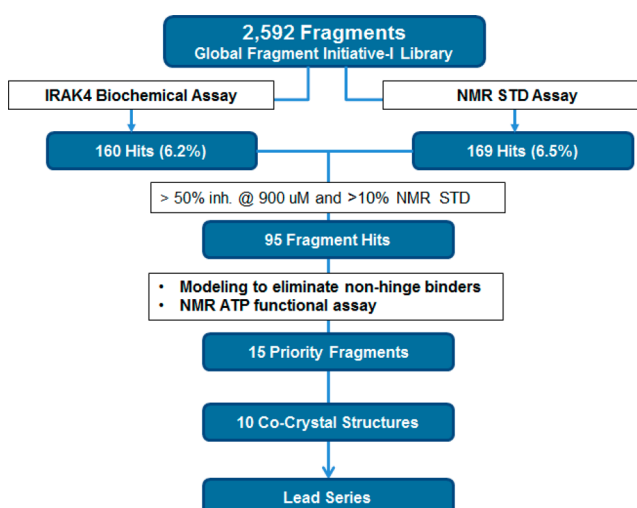


**Figure 3. Summary of the IRAK4 fragment screen.**

Among the 10 compounds for which co-crystal structures were obtained, we were particularly attracted to carboxamide **51**. Carboxamide **51** offers relatively potent activity for IRAK4, with an IC<sub>50</sub> of 55 μM in an enzymatic assay employing full-length IRAK4 at 600 μM ATP, which translated to highly encouraging values for the quality metrics ligand efficiency (LE, 0.46) and fit quality (FQ, 0.9), albeit with a modest lipophilic efficiency (LipE)<sup>47,48</sup> of 2.7. We were intrigued as well by the binding mode of **51**: X-ray crystallography indicated that **51** makes an intramolecular hydrogen bond between the ether oxygen and the amide to afford a pseudobicyclic fused ring system which can engage IRAK4 with the carboxamide acting as a two-point hinge binding motif to Met265 and Val263. The isopropyl ether appears to be close enough to the gatekeeper Tyr262, within approximately 3.5 Å, to make van der Waals interactions (Figure 4).

While carboxamide **51** offered an attractive starting point for medicinal chemistry efforts, its potency at IRAK4 was clearly several orders of magnitude weaker than would be required for a

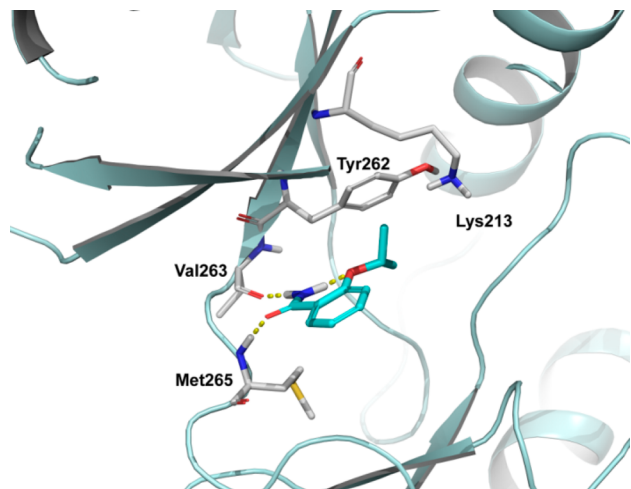


**Figure 4.** Co-crystal structure of compound **51** with IRAK4, highlighting interactions of compound **51** with Met265 and Val263 in the hinge region and with gatekeeper Tyr262.

drug candidate. We elected to adopt a fragment growing strategy, and rather than optimize potency alone, we aimed to simultaneously increase potency and LipE while maintaining a high LE in order to optimize pharmacological and oral pharmacokinetic properties. Given that our chosen fragment hit has a rather flat topology, our goal was to fully utilize available three-dimensional space within the IRAK4 ATP site. Encouraged by an analysis by Lovering et al. indicating that compared to leads, drugs tend to have an increased percentage of  $sp^3$  carbon atoms,<sup>49</sup> we made incorporation of increased  $sp^3$  character, chirality, and/or three-dimensional topology a further aim of our optimization efforts.

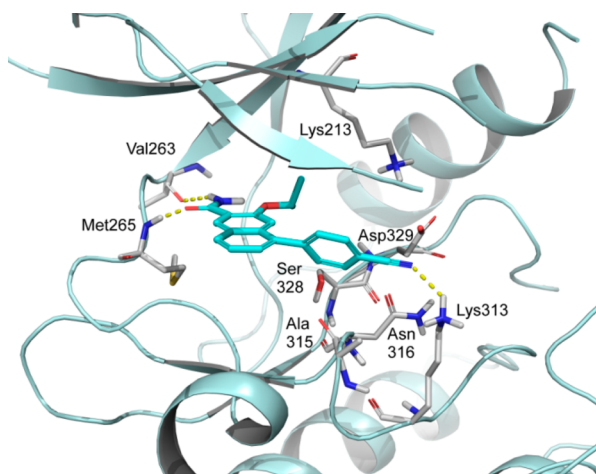
Inspection of carboxamide **51** bound to IRAK4 suggested the potential to grow the fragment further toward the front of the ATP pocket. In our initial attempts to more completely occupy the ATP binding site and eventually build toward polar residues such as Asp329, Asn316, and Ala315, we expanded the core to afford naphthalene **10** and were delighted to observe a greater than 30-fold improvement in potency, which was achieved with detriment to neither LE nor LipE. Various trajectories from the

**Table 1.** Elaboration of Benzamide Fragment Hit **51** to Isoquinoline **16**

Cpd	Structure	IRAK4 IC <sub>50</sub> (nM) <sup>a</sup>	cLogP	LE	LipE
<b>51</b>		55,056	1.6	0.45	2.7
<b>10</b>		2,087 <sup>b</sup>	2.8	0.46	2.9
<b>12</b>		71.9 <sup>b</sup>	4.1	0.39	3.0
<b>14</b>		146 <sup>b</sup>	2.6	0.39	4.2
<b>16</b>		121	2.8	0.40	4.1

<sup>a</sup>All experiments to determine IC<sub>50</sub> values were performed in at least duplicate at each compound concentration dilution unless otherwise noted, and the geometric mean of all of the IC<sub>50</sub> values is provided when the IC<sub>50</sub> was determined from two or more independent experiments, <sup>b</sup>n = 1.

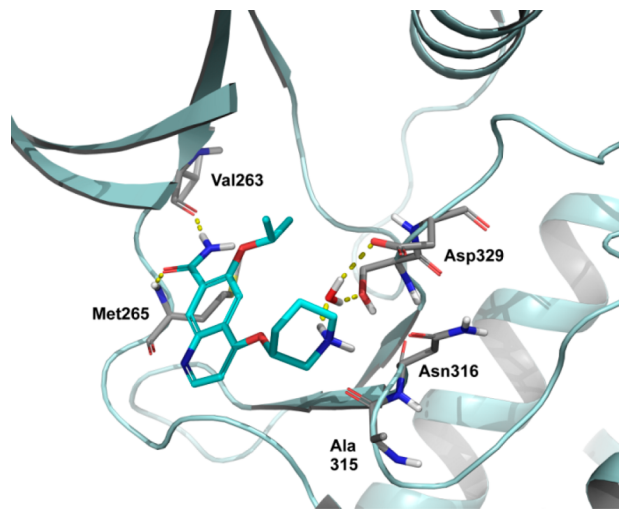
naphthalene were considered for building additional binding interactions. Naphthalene derivative **12** was found to offer a dramatically increased potency of 71.9 nM, again with comparable LE and LipE (Table 1). While **12** validated a productive vector from which to elaborate our fragment hits, its flat topology and high lipophilicity suggested additional structural modifications would be required before undertaking further fragment growth (Figure 5). We noticed that the



**Figure 5.** Co-crystal structure of **12** with IRAK4, highlighting the proximity of the cyano moiety to Lys313 and the presence of polar residues in this region such as Asp329 and Ser328, which are not engaged.

naphthalene ring distal to the hinge binding groups appeared to be surrounded by water molecules and thus hypothesized that it might be possible to replace the naphthalene with a more polar heterocyclic system. This was indeed the case, and we were quickly able to demonstrate that the core ring system could be switched to a quinoline with minimal change in activity (data not shown). The quinoline offered a further advantage in facilitating additional chemistries for exploring fragment growth tactics. The growth vector validated by **12** indicated opportunities to increase potency by engaging residues such as Ala315, Asn316, Ser328, and Asp329 (Figure 5). Piperidine ether **14** rapidly emerged as a promising lead from a small library of analogues probing this vector using S<sub>N</sub>Ar chemistry (Scheme 1). This compound displayed a 1.5 unit improvement in LipE and a significant increase in potency against IRAK4 enzyme as compared to fragment hit **51** (Table 1). Through **16**, we were able to show that isoquinoline functioned at least as effectively as quinoline for the core ring. Furthermore, this change had the effect of improving membrane permeability, as measured in an RRCK assay,<sup>50</sup> with **14** affording an apparent permeability ( $P_{app}$ ) of  $2.8 \times 10^{-6}$  cm/s and **16** affording  $P_{app}$  of  $11.4 \times 10^{-6}$  cm/s. This improvement in permeability arises presumably through attenuation of basicity and polarity of the heterocyclic system, as the Log D of **14** is 0.4 while that of **16** is 0.7.

A co-crystal structure of **14** in the kinase domain of IRAK4 (Figure 6) illustrates the same hinge contacts and placement of the core ring structure as in our original fragment hit, with the piperidine occupying the ribose binding region of the ATP site. The protonated basic center of the piperidine is in proximity to the backbone carbonyls of Ala315 and Asn316, and makes water-mediated hydrogen bonding interactions to Ser328 and Asp329.

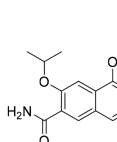
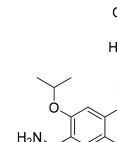
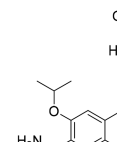
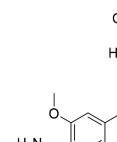
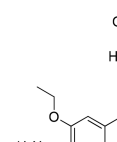
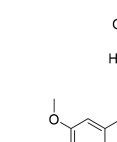
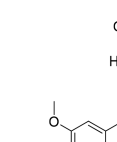


**Figure 6.** Co-crystal structure of **14** in IRAK4 has the piperidine nitrogen in proximity to the backbone carbonyls Ala315 and Asn316 and shows water-mediated hydrogen bonding interactions to Ser328 and Asp329.

While **16** provided a large step forward toward our goal, analysis of the protein–ligand complex for this molecule suggested further opportunities for potency enhancement through the optimization of interactions with residues at the base of the ribose pocket, for example, Ser328. A parallel medicinal chemistry library of compounds was designed to target polar interactions with residues in this region, and this effort led to the identification of five-membered lactam **20** as a breakthrough compound with single-digit nanomolar potency against IRAK4 enzyme and a two-unit increase in LipE versus the corresponding piperidine **16** (Table 2). The corresponding (*R*)-enantiomer, **24**, was found to be significantly less potent than the (*S*)-enantiomer **20**. X-ray crystallography showed that **20** binds to IRAK4 with the lactam NH acting as a hydrogen bond donor to the backbone carbonyls of Ala315 and Asn316, while the lactam carbonyl accepts hydrogen bonds from Ser328 and a water-mediated interaction with Lys213 (Figure 7). In addition, a water-mediated interaction is observed between the isoquinoline core nitrogen and Asp272.

Having made this advance through optimization of polar interactions deep into the ribose pocket, we turned next to optimization of the C-7 ether position which interacts with the gatekeeper residue, Tyr262, in a relatively rigid region of IRAK4. Methyl ether **21** proved to be roughly equipotent to isopropyl ether **20** despite being almost a whole unit less lipophilic (thus providing an increase in LipE), while ethyl ether **22** was less potent (Table 2). Compounds **23** and **26** illustrate that optimization tactics employed in both the ribose pocket and at C-7 were compatible with modification of the core ring system to a quinoline or naphthalene. Consistent with earlier findings, the quinoline system proved to be more polar, which had a modest negative impact upon permeability, while the naphthalene system was more lipophilic, with compound **26** displaying a Log D 1.5 compared to the Log D of 0.9 for the corresponding isoquinoline **21**. Consistent with the increased lipophilicity of naphthalene **26**, a modest negative impact upon metabolic stability as assessed in human liver microsomes (HLM) was observed. At this point, in addition to further ADME profiling, lead compounds were assessed for IRAK4 cell potency by measuring R848-stimulated TNF $\alpha$  production in PBMCs

Table 2. Identification of Lactam Substituent and SAR of Core and Ether Moieties

Cpd	Structure	IRAK4 IC <sub>50</sub> (nM) <sup>a</sup>	cLogP	LE	LipE	PBMC IC <sub>50</sub> (nM) <sup>a</sup>	HLM Cl <sub>int, app</sub> (μL/min/mg)	RRCK Papp AB (10 <sup>-6</sup> cm/s)
16		121	2.8	0.40	4.1	1,552 <sup>b</sup>	11	11.4
20		4.6	1.7	0.46	6.6	133	10	10.7
24		840 <sup>b</sup>	1.7	0.33	4.4	NT	NT	10.5
21		7.6	0.9	0.48	7.2	347	9	9.9
22		23.9	1.4	0.44	6.2	672	9	10.6
23		5.9	0.7	0.49	7.6	2,118	<8	5.8
26		1.3 <sup>b</sup>	1.0	0.53	7.9	37.1	13	14.2

<sup>a</sup>All experiments to determine IC<sub>50</sub> values were performed in at least duplicate at each compound concentration dilution unless otherwise noted, and the geometric mean of all of the IC<sub>50</sub> values is provided when IC<sub>50</sub>s were determined from two or more independent experiments. <sup>b</sup>n = 1. NT: not tested.

isolated from human blood. As a result of this profiling, we found that compounds bearing the isoquinoline core generally offered the best balance of IRAK4 pharmacology in enzyme and cell assays and ADME properties.

Having improved IRAK4 potency by greater than 4 orders of magnitude and optimized the ADME properties of our IRAK4 inhibitors, we proceeded to more fully characterize one of our lead molecules. The selectivity profile of lactam 20 was assessed

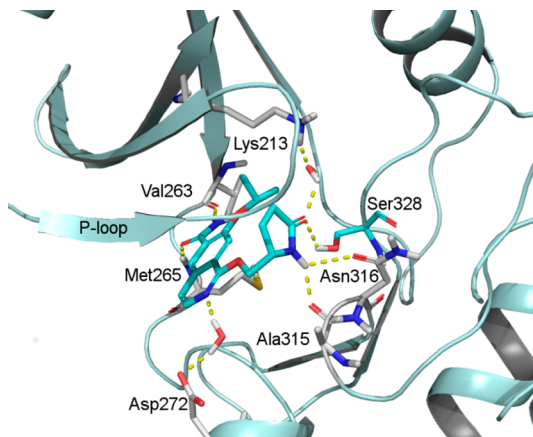


Figure 7. Co-crystal structure of compound 20 with IRAK4.

using the KiNativ method (ActivX) in THP1 cell lysates, and 20 was found to be highly selective for IRAK4 (Figure 8). Lactam 20 was evaluated for off-target pharmacological activity in a panel of receptors, ion channels, transporters, and enzymes (64 targets in total) in a wide ligand profile screen (CEREP) at 10  $\mu$ M and found to have inhibited no targets at >50%. The human ether-a-go-go-related gene (hERG) IC<sub>50</sub> of 20 was greater than 30  $\mu$ M, indicating a low risk of QT prolongation. The ability of compound 20 to inhibit five major CYP450 enzymes was assessed using pooled human liver microsomes and probe substrates for the CYP450 enzymes.<sup>51</sup> At a concentration of 3  $\mu$ M of compound 20, less than 10% inhibition of CYPs 1A2, 2C8, 2D6, and 3A4, and 13.6% inhibition of CYP2D9 was observed, suggesting a low risk of drug–drug interaction for this IRAK4 inhibitor. The thermodynamic solubility of crystalline 20 at pH 6.5 was determined to be 78  $\mu$ M.

Lactam 20 was found to have an intravenous (iv) clearance of 23 mL/min/kg, a half-life of 1.2 h, and an oral bioavailability of 57% in rat. The fraction unbound in plasma protein of 20 is 29% and 21% in human and rat, respectively. With this favorable selectivity and pharmacokinetic profile in hand, in vivo efficacy of 20 was assessed using oral administration in a rat collagen induced arthritis (CIA) model in therapeutic mode, i.e., with compound treatment being initiated after rats developed disease. Lactam 20 led to a significant reduction in paw swelling vs vehicle at 30 and 100 mg/kg BID (Figure 9). Spleens from the rats in this study were subjected to KiNativ analysis (ActivX), and dose-dependent, selective engagement of IRAK4 was observed from samples obtained at 1 h postdose, corresponding to the approximate C<sub>max</sub> (Figure 9). At this time point, the 100 mg/kg dose led to approximately 80% receptor occupancy of IRAK4.

While 20 represented an important advance for the program, preliminary human dose projections suggested this compound did not possess sufficient potency to be considered further. We began further optimization efforts from methyl ether analogue 21, which had a similar rat pharmacokinetic profile to 20, with an iv clearance of 35 mL/min/kg, a 1 h half-life, and an oral

bioavailability of 44% F, while offering improved LE and LipE compared to the isopropyl ether analogue 20.

Further analysis of a co-crystal structure of 20 with IRAK4 using Watermap<sup>52,53</sup> suggested a high energy water positioned between the lactam ring and the P-loop, as illustrated in Figure 10. The thermodynamic signature of the putative water ( $\Delta G = 9.12$ ,  $-T\Delta S = 1.16$ ,  $\Delta H = 7.96$ ) suggests a significant contribution to its energy from enthalpy. In addition, it was hypothesized that the unshielded hydrogen bond between glycines 195 and 198 in the P-loop may comprise a dehydron.<sup>54</sup> Shielding of such dehydrons may afford an increase in potency.<sup>55</sup> Moreover, this is one of the few trajectories from the ligand that would probe unexplored space that does not point toward bulk solvent. To this end, compounds were designed that explored substitution at the lactam position beta to the carbonyl, increasing the fraction sp<sup>3</sup> and further reducing the planar topology of the molecules.

As had been anticipated, this structural change led to increased potency in enzyme and cellular assays with the effect being particularly pronounced for the 3-ethyl derivative 31 with a 30× increase in potency in the cell assay (Table 3). Larger substituents were less effective, as illustrated by analogues such as 32, which had reduced LipE compared to 31, and 33, which offered lower enzyme and cell potency.

Further modification of the lactam was undertaken to improve cell potency as measured in the PBMC assay; the lower limit of the enzyme assay was reached with IC<sub>50</sub> values below 1 nM. Analysis of the protein crystal structure of 20 suggested there may be sufficient space to accommodate a small substituent at the 4-position. Introduction of a methyl substituent *syn* to the 3-methyl substituent led to a substantial loss in potency, as shown in 36, while the *anti* dimethyl analogue 37 was tolerated from a potency standpoint (Table 3), but this led to lower LE and LipE values and, as expected, HLM clearance was increased. Fused cyclopropane systems were also explored as a means to achieve potency through a similar interaction with the P-loop while minimizing the negative impact on metabolic stability from increased lipophilicity relative to 21. Cyclopropanes 44 and 45 provided potency similar to the 3-methyl analogue 30 with excellent metabolic stability.

Addition of a fluorine substituent to the  $\alpha$  position of the lactam, as in compound 38 (PF-06426779<sup>37</sup>) and compounds 39–41, was found to consistently afford increased potency compared to the corresponding *des*-fluoro analogues as measured in both enzyme and cell assays. This further increase in potency upon fluorine substitution was observed in the cyclopropanes as well, e.g., 50, but overall the cyclopropane series proved less potent than those analogues with the 3-ethyl substituent. Furthermore, the relative stereochemistry of the fluorine substituent was found to have an impact, with *syn* stereochemistry to the ether linker preferred for potency, e.g., compound 38 vs compound 39. We hypothesize that the increased potency conferred by fluoro substitution may be due to increased hydrogen bond donor capability of the lactam. In

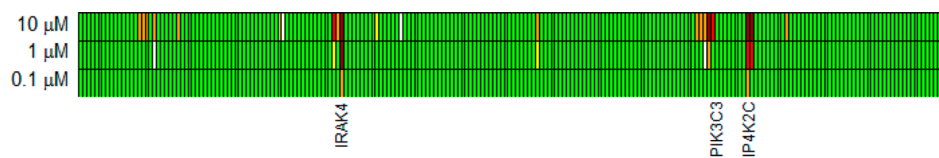
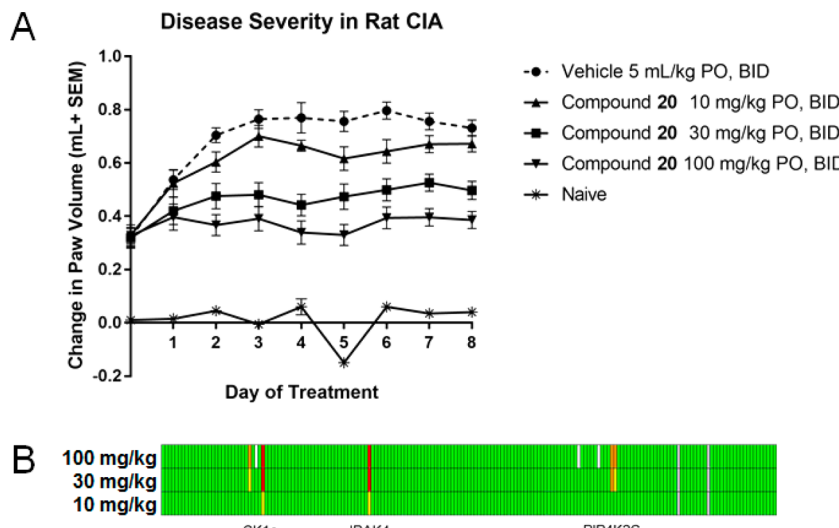
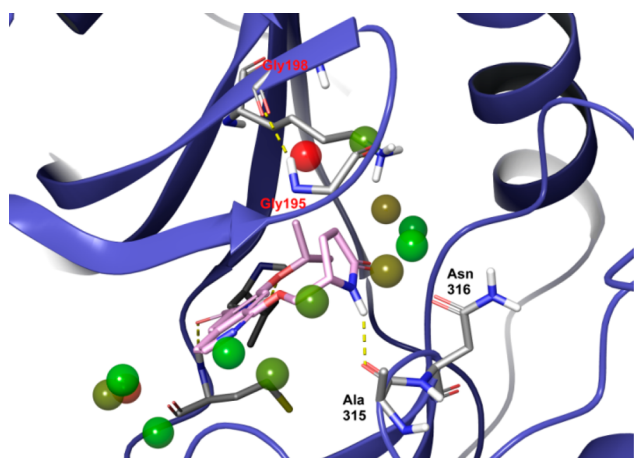


Figure 8. Kinase selectivity of compound 20 in THP1 cell lysates using KiNativ method (ActivX).



**Figure 9.** (A) Change in paw volume versus time of compound 20 in a rat collagen induced arthritis (CIA) model. (B) Kinase profile via KiNativ analysis (ActivX) of rat spleen samples from the CIA study.



**Figure 10.** Watermap and dehydron analysis of compound 20. A high-energy water molecule (red) is shown close to a dehydron in the P-loop.

agreement with the hypothesis that introduction of a substituent targeting the high energy water and dehydron discussed previously would lead to increased potency, compound 40 (PF-06650833)<sup>37,56</sup> emerged as the most potent compound from our efforts to optimize substitution around the lactam moiety, with an IC<sub>50</sub> of approximately 2 nM in the PBMC assay as well as in a human whole blood assay when corrected for plasma protein binding. The X-ray structure of this compound bound to IRAK4 is shown in Figure 11A, illustrating the key interactions established through the fragment optimization campaign. Figure 11B displays a small molecule X-ray structure of compound 40; it will be seen that the conformation of 40 in the small molecule X-ray is strikingly similar to that of 40 in the enzyme bound state.

On the basis of its exceptional pharmacology profile and encouraging in vitro ADME profile, 40 was selected for detailed study.

Compound 40 is a crystalline solid with a melting point of 226 °C. Its solubility is 57 µg/mL in phosphate buffered saline at pH 6.7, with similar values in unbuffered water at pH 8.1 and simulated fasted state intestinal fluid at pH 6.5 (65 and 62 µg/mL, respectively).

Single-dose pharmacokinetic studies with compound 40 were conducted after iv and oral (po) administration to male rats, dogs, and monkeys (Table 4). After iv administration, compound 40 demonstrated high plasma clearance (CL) in rats and a low plasma CL in dogs and monkeys, with a moderate volume of distribution ( $V_{ss}$ ) in all species. Compound 40 was rapidly absorbed with low to moderate oral bioavailability in rats, dogs, and monkeys.

The kinase selectivity profile of compound 40 was assessed in a panel of 278 kinases (Invitrogen) at 200 nM inhibitor concentration using the ATP K<sub>m</sub> for each kinase. Approximately 100% inhibition was observed for IRAK4, while greater than 70% inhibition was observed for the following kinases, in order of potency: IRAK1, MNK2, LRRK2, CLK4, and CK1 $\gamma$  (see Supporting Information). Also, compound 40 was subjected to a KiNativ kinase screen (ActivX) in THP1 cell lysates at concentrations of 10, 50, 200, 1000, and 5000 nM to assess kinase selectivity under more physiological conditions. Of the approximately 270 unique kinases profiled, only these kinases other than IRAK4 displayed greater than 50% inhibition at 200 nM: CK1 $\gamma$ 2, IRAK3/M, PIPK2C, and CK1 $\delta/\epsilon$ . The high degree of kinase selectivity of compound 40 is typical of compounds in this chemical series.

Lactam 40 was evaluated in a wide ligand profile screen (CEREP) at an initial concentration of 10 µM. At this concentration, 40 demonstrated activity against VEGFR2 (KDR) kinase (activity defined by a response greater than 50% of a maximal response). A follow up concentration-response curve was generated, and the VEGFR2 IC<sub>50</sub> value was determined to be 5330 nM. Lactam 40 was subsequently assessed in a whole cell functional VEGF2R assay (PAE-KDR cell line). No activity was observed at concentrations up to and including 30 µM. In a voltage clamp assay, 40 inhibited hERG current by 25% at 100 µM.

The ability of compound 40 to inhibit five major CYP450 enzymes was assessed using pooled human liver microsomes and probe substrates for the CYP450 enzymes.<sup>51</sup> At a concentration of 3 µM of compound 40, less than 5% inhibition of CYPs 1A2, 2C8, 2C9, 2D6, and 3A4 was observed. Lactam 40 was examined for time dependent inhibition effects on six major CYP450 enzymes (CYP1A2, 2B6, 2C8, 2C9, 2C19, and 2D6) using

Table 3. Optimization of Lactam

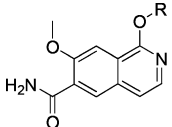
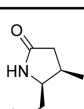
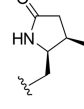
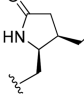
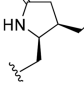
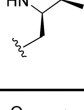
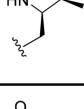
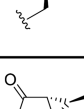
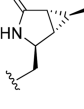
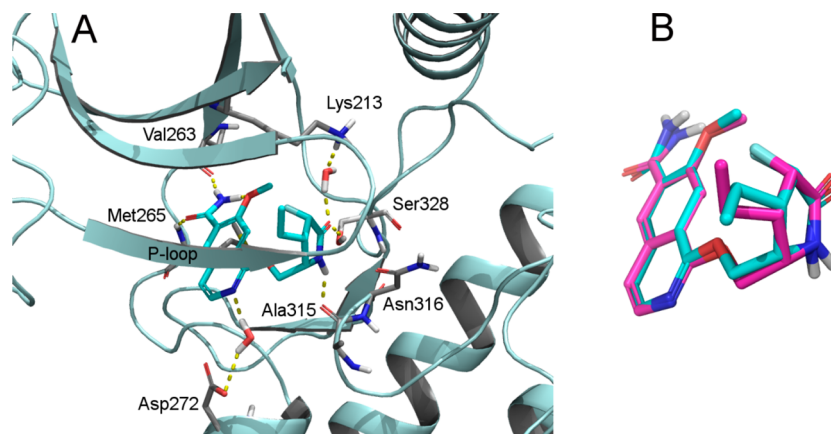
Cpd	R	IRAK4 IC <sub>50</sub> (nM) <sup>a</sup>	cLogP	LE	LipE	PBMC IC <sub>50</sub> (nM) <sup>a</sup>	HLM Cl <sub>int,</sub> app (μL/min/mg)	RRCK Papp AB (10 <sup>-6</sup> cm/s)
21		7.6	0.9	0.48	7.2	347	9	9.9
30		2.7	1.4	0.49	7.2	52.3	<9	10.5
31		0.5	1.9	0.51	7.4	9.0	14	17.9
32		1.3	2.4	0.47	6.4	28.4	44	18.9
33		12.1 <sup>b</sup>	0.1	0.42	7.8	373	<8	12.5
36		29.2 <sup>b</sup>	1.8	0.41	5.6	2,836 <sup>b</sup>	9	15.8
37		3.7 <sup>b</sup>	1.9	0.46	6.5	87.1	32	13.9
44		4.8	1.9	0.48	7.5	115	<8	11.7
45		2.4	1.4	0.47	7.2	52.1	<8	13.5

Table 3. continued

Cpd	R	IRAK4 IC <sub>50</sub> (nM) <sup>a</sup>	cLogP	LE	LipE	PBMC IC <sub>50</sub> (nM) <sup>a</sup>	HLM Cl <sub>int,</sub> app (μL/min/mg)	RRCK Papp AB (10 <sup>-6</sup> cm/s)
<b>38</b>		0.3	1.7	0.52	7.8	12.7	<9	9.9
<b>39</b>		1.9	1.7	0.48	7.0	29.5	12	10.4
<b>40</b>		0.2	2.2	0.51	7.4	2.4	25	9.6
<b>41</b>		0.1	2.2	0.52	7.6	6.5	15	14.2
<b>50</b>		0.6	1.4	0.49	7.8	16.8	<8	16.3

<sup>a</sup>All experiments to determine IC<sub>50</sub> values were performed in at least duplicate at each compound concentration dilution unless otherwise noted, and the geometric mean of all of the IC<sub>50</sub> values is provided when IC<sub>50</sub>s were determined from two or more independent experiments. <sup>b</sup>n = 1.



**Figure 11.** (A) Co-crystal structure of **40** with IRAK4 kinase domain. (B) Overlay of bound conformation of **40** in IRAK4 kinase domain (cyan) and small molecule crystal structure of **40** (magenta).

pooled human liver microsomes and probe substrates. At 100 μM of **40**, no time dependent CYP inhibition was observed. The potential induction of CYP3A by **40** was assessed using cryopreserved human hepatocytes and afforded a 4.4-fold increase in mRNA at 10 μM. These data suggest a low risk of potential drug–drug interactions.

In vivo activity of compound **40** was assessed in the rat systemic LPS induced TNFα model. Male Sprague–Dawley rats

were first dosed po with compound at 0.3, 1, 3, and 30 mg/kg. At 1 h post dosing, the animals were challenged with LPS intravenously, and blood was collected 1.5 h post challenge and assayed for TNF. Compound **40** significantly inhibited LPS-induced TNF in a dose dependent manner (**Figure 12**). Mean exposures of compound **40** in plasma were 2.1, 7.7, 19, and 150 nM free, respectively, at 2.5 h after oral administration of

**Table 4. In Vivo Pharmacokinetic Profile of Compound 40 in Rat, Dog, and Monkey<sup>a</sup>**

species	dose (mg/kg)	route	t <sub>1/2</sub> (h)	CL, p (mL/min/kg)	V <sub>ss</sub> (L/kg)	F (%)
rat	1 <sup>b</sup>	iv	0.6	56	1.8	NA <sup>f</sup>
rat	5 <sup>c</sup>	po	1.4– 2.1	NA	NA	34–50
dog	1 <sup>d</sup>	iv	1.1	10	0.77	NA
dog	5 <sup>e</sup>	po	4.0	NA	NA	41
monkey	1 <sup>d</sup>	iv	1.7	10	0.95	NA
monkey	5 <sup>e</sup>	po	6.2	NA	NA	6.9

<sup>a</sup>Male Wistar-Han rats, male beagle dogs, and male cynomolgus monkey were used in these studies. <sup>b</sup>Vehicle was 10% DMSO/30% PEG400 in water. <sup>c</sup>Vehicle was 0.5% methylcellulose in water. <sup>d</sup>Vehicle was 10% DMSO/60% PEG400 in water. <sup>e</sup>Compound 40 was milled, and vehicle was 1.25% hydroxypropyl cellulose and 0.05% docusate sodium salt in water. <sup>f</sup>NA = not applicable.

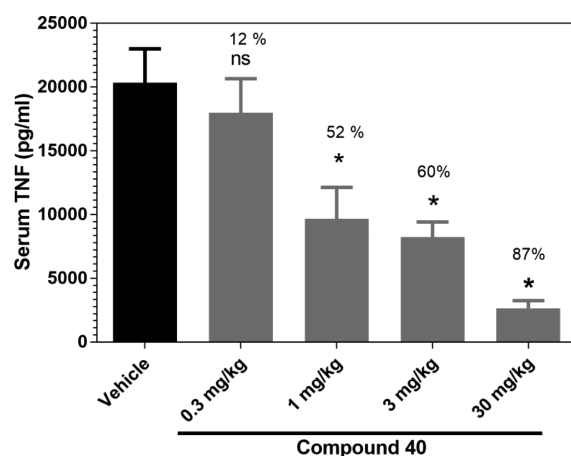


**Figure 12.** Dose-response of compound 40 in the acute LPS challenge model in rat.

compound 40 at 0.3, 1, 3, and 30 mg/kg. The fraction unbound in rat plasma of compound 40 is 0.3.

Compound 40 was designed to leverage the relatively compact ATP-binding site of IRAK4 and delivers excellent potency in a full-length IRAK4 enzyme assay and more physiologically relevant cellular assays. As a molecule with a moderate molecular weight (361 g/mol), and reasonable heavy atom count and lipophilicity (measured Log D of 2.0), this potency translates to high LE and LipE. Compound 40 contains a lactam bearing three contiguous chiral centers which allow for efficient engagement of key polar residues beyond the ribose binding region and the P-loop of IRAK4; this molecular complexity of 40 was realized

through conjugate addition and subsequent alkylation of a key lactam acetonide intermediate derived from pyroglutamic acid. The kinase selectivity of 40 in enzymatic and cellular assays was found to be excellent, and low promiscuity was observed in broad ligand profiling. Lactam 40 has favorable in vitro and in vivo ADME profiles and demonstrates oral efficacy as exemplified by the inhibition of serum TNF secretion in an acute setting in rat. These data, together with in vitro safety data, supported the advancement of this compound into clinical development.

## CONCLUSION

In summary, compound 40 and other compounds in this chemical series are the result of a fragment-based drug discovery effort in which structure-based drug design enabled optimization of the series to deliver IRAK4 inhibitors with exquisite enzyme and cellular potency, ligand efficiency, and lipophilic efficiency (Figure 13). These compounds offer excellent kinase selectivity and ADME properties. The IRAK4 inhibitor 40 has advanced to clinical trials, the results of which will be reported in due course.

## EXPERIMENTAL SECTION

**General Experimental Methods.** Reagents and solvents were obtained from Aldrich and/or Alfa and were used without further purification. Solvents were commercial anhydrous grades and were used as received. All reactions were conducted with continuous magnetic stirring under an atmosphere of dry nitrogen unless otherwise specified.

All new compounds were characterized by proton (<sup>1</sup>H) NMR spectra using Bruker spectrometers and are reported in parts per million (ppm) relative to the residual resonances of the deuterated solvent. Carbon (<sup>13</sup>C) and fluorine (<sup>19</sup>F) NMR spectra were recorded similarly. All <sup>13</sup>C NMR and <sup>19</sup>F NMR spectra were proton decoupled. Infrared spectra were recorded on a Nicolet Avatar 370 FT-IR and are reported in reciprocal centimeters (cm<sup>-1</sup>). Melting points were obtained on a Thomas-Hoover Mel-Temp capillary melting point apparatus and are uncorrected. Elemental analyses were performed by Intertek, 291 Route 22 East, PO Box 470, Whitehouse, NJ 08888, USA.

Low-resolution mass spectrometry analyses were conducted on Waters Acuity UPLC and SQ systems. Signal acquisition conditions included: Waters Acuity HSS T3 C18 2.1 50 mm column at 60 °C with 0.1% formic acid in water (v/v) as the mobile phase A, 0.1% formic acid in acetonitrile (v/v) as the mobile phase B; 1.25 mL/min as the flow rate and ESCI (ESI±, APCI±), 100–2000m/z scan, 0.4 s scan time, Centroid as the MS method. High-resolution mass spectrometry analyses were conducted on an Agilent 6220 TOF mass spectrometer in positive or negative electrospray mode. The system was calibrated to greater than 1 ppm accuracy across the mass range prior to analyses. The samples were separated using UHPLC on an Agilent 1200 system prior to mass spectrometric analysis. HPLC was carried out on an Xbridge C18 2.1 mm × 50 mm column at 50 °C with 0.0375% TFA in water (v/v) as the mobile phase A, 0.01875% TFA in acetonitrile (v/v) as the mobile phase B, and 0.80 mL/min as the flow rate.

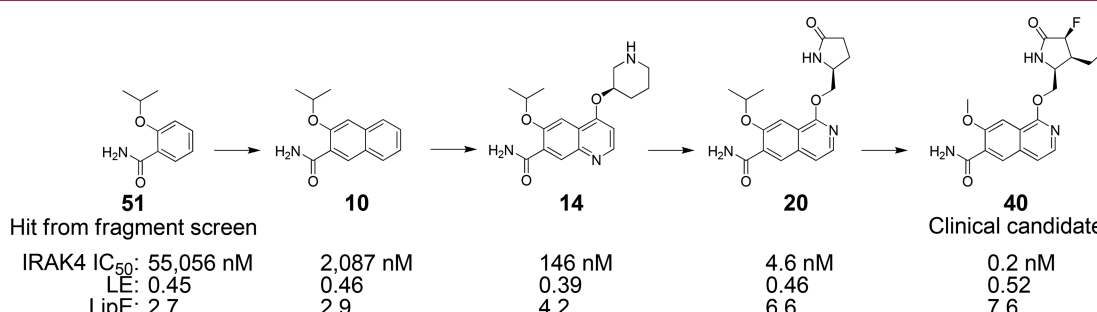


**Figure 13.** Optimization of fragment screening hit 51 to clinical candidate 40.

Flash chromatography was carried out on ISCO or Biotage purification systems using prepacked ISCO brand silica gel cartridges using an appropriate heptane–ethyl acetate solvent gradient unless otherwise specified. Analytical thin layer chromatography (TLC) was performed on 60 F254 glass plates precoated with a 0.25 mm thickness of silica gel purchased from EMD.

Purity of final compounds was assessed by elemental analysis for C, H, and N or by reversed-phase HPLC with UV detection at 255 nm. All tested compounds returned combustion analyses within 0.4% of theoretical values or demonstrated HPLC purity >95%, unless otherwise noted.

**3-Isopropoxy-2-naphthamide (10).** 3-Hydroxy-2-naphthamide<sup>57</sup> (9, 200 mg, 1.1 mmol) and K<sub>2</sub>CO<sub>3</sub> (520 mg, 3.8 mmol) were combined in DMSO (3 mL) and treated with 2-iodopropane (0.13 mL, 1.3 mmol). The reaction vessel was sealed and heated at 130 °C for 2 h. Water (50 mL) was added, and the mixture was extracted with DCM. The DCM was washed with water and brine, dried over Na<sub>2</sub>SO<sub>4</sub>, filtered, and concentrated. The residue was purified by chromatography to afford 226 mg (92%) of **10** as a white solid; mp 128–130 °C. <sup>1</sup>H NMR (400 MHz, DMSO-*d*<sub>6</sub>) δ 8.39 (s, 1 H), 7.95 (d, *J* = 8.20 Hz, 1 H), 7.86 (d, *J* = 8.20 Hz, 1 H), 7.71 (br s, 1 H), 7.64 (br s, 1 H), 7.52 (m, 1 H), 7.50 (s, 1 H), 7.40 (*t*, *J* = 7.00 Hz, 1 H), 4.83–4.84 (m, 1 H), 1.42 (d, *J* = 5.85 Hz, 6 H). <sup>13</sup>C NMR (101 MHz, DMSO-*d*<sub>6</sub>) δ 166.99, 153.06, 135.70, 131.89, 128.93, 128.20, 127.87, 126.84, 126.02, 124.71, 109.31, 71.39, 40.69, 40.27, 39.85, 39.44, 22.17. LCMS: 230 (MH<sup>+</sup>). HRMS: calcd mass for C<sub>14</sub>H<sub>15</sub>NNaO<sub>2</sub> (M + Na<sup>+</sup>) 252.0995; found 52.1006; difference 4.34 ppm. Analysis: Calcd for C<sub>14</sub>H<sub>15</sub>NNaO<sub>2</sub>: C, 73.34%; H, 6.59%; N, 6.11%. Found: C, 72.95%; H, 6.42%; N, 5.91%. HPLC purity: 95.39%.

**5-(4-Cyanophenyl)-3-isopropoxy-2-naphthamide (12).** A solution of 5-hydroxy-3-isopropoxy-2-naphthamide<sup>37</sup> (11, 200 mg, 0.82 mmol) in THF (5 mL) was treated with NaH (60% in oil, 34 mg, 0.82 mmol) at 45 °C and stirred for 30 min, then cooled to 20 °C. A solution of N-phenylbis(trifluoromethanesulfonimide) (293 mg, 0.82 mmol) in THF (2 mL) was added, and the reaction mixture was stirred at 20 °C for 1 h before being diluted with EtOAc and water. The EtOAc was dried (Na<sub>2</sub>SO<sub>4</sub>) and concentrated to give the intermediate triflate (250 mg, 80%) as a pale-orange solid, which was used immediately without further purification. A suspension of the triflate (60 mg, 0.16 mmol) and 4-cyanophenylboronic acid (28 mg, 0.19 mmol) in toluene (1.5 mL) and ethanol (0.5 mL) was treated with 2 M Na<sub>2</sub>CO<sub>3</sub> (0.2 mL), placed under N<sub>2</sub>, and Pd(PPh<sub>3</sub>)<sub>4</sub> (19 mg, 0.03 mmol) added. The reaction mixture heated under reflux for 2 h before being diluted with EtOAc and water. The EtOAc extract was washed with brine, dried over Na<sub>2</sub>SO<sub>4</sub>, filtered, and concentrated. The residue was purified by chromatography to provide 50 mg (90%) of **12** as a white solid; mp 235–238 °C. <sup>1</sup>H NMR (400 MHz, DMSO-*d*<sub>6</sub>) δ 8.50 (s, 1 H), 8.09–8.05 (m, 1 H), 8.03 (d, *J* = 8.2 Hz, 2 H), 7.75 (d, *J* = 8.2 Hz, 2 H), 7.70 (br s, 2 H), 7.54–7.49 (m, 2 H), 7.16 (s, 1 H), 4.56 (spt, *J* = 5.9 Hz, 1 H), 2.52 (br s, 1 H), 1.32 (d, *J* = 5.9 Hz, 6 H). <sup>13</sup>C NMR (101 MHz, DMSO-*d*<sub>6</sub>) δ 166.12, 153.02, 144.71, 136.12, 132.53, 132.19, 132.11, 130.59, 129.27, 128.90, 127.81, 125.76, 123.94, 118.79, 110.34, 106.01, 71.04, 21.35. LCMS: 331 (MH<sup>+</sup>). HRMS: calcd mass for C<sub>21</sub>H<sub>19</sub>NNaO<sub>2</sub> (MH<sup>+</sup>) 331.1441; found 331.1446; difference 1.4 ppm. Analysis: Calcd for C<sub>21</sub>H<sub>18</sub>NNaO<sub>2</sub>: C, 76.34%; H, 5.49%; N, 8.48%. Found: C, 75.99%; H, 5.47%; N, 8.35%.

**(R)-6-Isopropoxy-4-(piperidin-3-yloxy)quinoline-7-carboxamide (14).** KOtBu (4.37 g, 39 mmol) was added to a solution of (R)-N-Boc-3-hydroxypiperidine (3.82 g, 19 mmol) in DMSO (10 mL). The mixture was stirred at 20 °C for 10 min, after which a solution of 4-chloro-6-isopropoxyquinoline-7-carboxamide<sup>37</sup> (13, 5.03 g, 19 mmol) in DMSO (5 mL) was added dropwise to the reaction mixture. The reaction mixture was stirred at 60 °C for 4 h. The reaction mixture was then diluted with EtOAc and water, and the phases were separated. The aqueous phase was extracted three times with EtOAc, and the combined EtOAc extracts were dried (Na<sub>2</sub>SO<sub>4</sub>) and concentrated. The residue was purified by chromatography on silica gel, then dissolved in DCM (10 mL) and treated at 0 °C with TFA (7.9 mL). The mixture was stirred at 20 °C for 4 h then concentrated to dryness. The solid was triturated with Et<sub>2</sub>O and dried under vacuum to afford 7.20 g (94%) of **14** as a colorless solid; mp 199–202 °C (decomposes). <sup>1</sup>H NMR (400 MHz, DMSO-*d*<sub>6</sub>) δ 9.05 (d, *J* = 6.2 Hz, 1 H), 8.35 (s, 1 H), 7.90 (br s, 1 H), 7.86 (s, 1 H),

7.84 (br s, 1 H), 7.60 (d, *J* = 6.2 Hz, 1 H), 5.43–5.34 (m, 1 H), 5.04 (spt, *J* = 6.0 Hz, 1 H), 3.66–3.55 (m, 1 H), 3.55–3.44 (m, 1 H), 3.30 (s, 1 H), 3.13 (s, 1 H), 2.14–1.90 (m, 3 H), 1.87–1.74 (m, 1 H), 1.41 (*t*, *J* = 6.4 Hz, 6 H). <sup>13</sup>C NMR (101 MHz, DMSO-*d*<sub>6</sub>, free base) δ 166.21, 158.18, 152.02, 149.91, 143.72, 131.25, 129.39, 123.23, 103.10, 102.99, 73.13, 71.41, 49.52, 45.42, 29.45, 24.21, 21.48, 21.42. LCMS: 330 (MH<sup>+</sup>). HRMS: Calcd mass for C<sub>18</sub>H<sub>24</sub>N<sub>3</sub>O<sub>3</sub> (MH<sup>+</sup>) 330.1812; found 330.1828; difference 4.76 ppm. HPLC purity: 97.66%.

**(R)-7-Isopropoxy-1-(piperidin-3-yloxy)isoquinoline-6-carboxamide (16).** A suspension of (R)-N-Boc-3-hydroxypiperidine (195 mg, 0.97 mmol) and 1-chloro-7-isopropoxyisoquinoline-6-carbonitrile<sup>37</sup> (15, 251 mg, 1.0 mmol) in DMF (3.2 mL) was cooled in a –10 °C bath for 15 min, after which KHMDS (1 M in THF, 1.26 mL) was added in rapid drops. The cooling bath was removed, and the mixture was stirred at 20 °C for 30 min. The reaction mixture was then poured into a mixture of 10% (w/v) NaH<sub>2</sub>PO<sub>4</sub> solution and EtOAc with vigorous stirring. The EtOAc was separated, washed with water and brine, dried over Na<sub>2</sub>SO<sub>4</sub>, filtered, and concentrated. The residue was dissolved in DMSO (3.0 mL) and treated with K<sub>2</sub>CO<sub>3</sub> (705 mg, 5.1 mmol) followed by H<sub>2</sub>O<sub>2</sub> (30%, 0.43 mL, 7.1 mmol) added dropwise at 20 °C. The mixture was stirred for 2 h before Me<sub>2</sub>S (0.73 mL, 22.8 mmol) was added to scavenge residual H<sub>2</sub>O<sub>2</sub>. Stirring was continued for 30 min before the reaction was filtered through Celite. The filter was washed with DCM and EtOAc, and the filtrate was concentrated under high vacuum to remove DMSO. The residue was purified by chromatography to afford the N-BOC intermediate, which was dissolved in DCM (3 mL) and treated with TFA (3 mL). After 2 h at 20 °C, the mixture was concentrated and the residue was purified by reverse phase chromatography using a MeCN–water with NH<sub>4</sub>OH modifier. The resulting product was triturated with MTBE and filtered to afford 220 mg (65%) of **16** as a white solid. <sup>1</sup>H NMR (500 MHz, DMSO-*d*<sub>6</sub>) δ 3.18 (s, 1 H), 7.87 (d, *J* = 5.62 Hz, 1 H), 7.71 (br s, 1 H), 7.70 (br s, 1 H), 7.61 (s, 1 H), 7.37 (d, *J* = 5.87 Hz, 1 H), 5.18 (tt, *J* = 7.64, 3.73 Hz, 1 H), 4.87 (dquin, *J* = 12.07, 6.03, 6.03, 6.03 Hz, 1 H), 3.19 (d, *J* = 2.69 Hz, 1 H), 2.71–2.83 (m, 2 H), 2.58–2.67 (m, 1 H), 2.03–2.14 (m, 1 H), 1.67–1.80 (m, 2 H), 1.46–1.56 (m, 1 H), 1.39 (dd, *J* = 5.99, 1.83 Hz, 6 H). <sup>13</sup>C NMR (126 MHz, DMSO-*d*<sub>6</sub>) δ 166.38, 158.01, 153.16, 137.83, 131.71, 130.84, 128.87, 120.75, 114.63, 105.11, 71.37, 70.48, 49.72, 45.44, 29.72, 24.18, 21.50, 21.43. LCMS: 330 (MH<sup>+</sup>). HRMS: calcd mass for C<sub>18</sub>H<sub>24</sub>N<sub>3</sub>O<sub>3</sub> (MH<sup>+</sup>) 330.1812; found 330.1814; difference 0.44 ppm. HPLC purity: 96.95%.

**(S)-7-Isopropoxy-1-((5-oxopyrrololidin-2-yl)methoxy)isoquinoline-6-carboxamide (20).** This was prepared from **15** and (S)-5-(hydroxymethyl)-pyrrolidin-2-one according to the general procedure for the preparation of **40**; mp 212–213 °C. <sup>1</sup>H NMR (400 MHz, DMSO-*d*<sub>6</sub>) δ 8.20 (s, 1 H), 8.10 (s, 1 H), 7.87 (d, *J* = 5.9 Hz, 1 H), 7.74 (br s, 1 H), 7.72 (br s, 1 H), 7.64 (s, 1 H), 7.40 (d, *J* = 5.9 Hz, 1 H), 4.91 (spt, *J* = 5.9 Hz, 1 H), 4.47 (dd, *J* = 3.5, 10.9 Hz, 1 H), 4.31 (dd, *J* = 6.2, 10.9 Hz, 1 H), 4.03 (br s, 1 H), 2.38–2.12 (m, 3 H), 1.98–1.83 (m, 1 H), 1.40 (*t*, *J* = 6.6 Hz, 6 H). <sup>13</sup>C NMR (101 MHz, DMSO-*d*<sub>6</sub>) δ 177.11, 166.38, 158.47, 153.25, 137.65, 131.58, 130.85, 128.88, 120.32, 115.14, 105.08, 71.21, 69.16, 52.31, 29.71, 22.94, 21.64, 21.41. LCMS: 344 (MH<sup>+</sup>). HRMS: calcd mass for C<sub>18</sub>H<sub>21</sub>N<sub>3</sub>NaO<sub>4</sub> (M + Na<sup>+</sup>) 366.1424; found 366.144; difference 4.21 ppm. Analysis: Calcd for C<sub>18</sub>H<sub>21</sub>N<sub>3</sub>O<sub>4</sub>: C, 62.96%; H, 6.16%; N, 12.24%. Found: C, 62.97%; H, 6.23%; N, 12.29%. HPLC purity: 97.10%.

**(S)-7-Methoxy-1-((5-oxopyrrololidin-2-yl)methoxy)isoquinoline-6-carboxamide (21).** This was prepared from **17** and (S)-5-(hydroxymethyl)-pyrrolidin-2-one according to the general procedure for the preparation of **40**; mp 215–217 °C. <sup>1</sup>H NMR (500 MHz, DMSO-*d*<sub>6</sub>) δ 8.16 (s, 1 H), 8.13 (br s, 1 H), 7.92–7.87 (m, 1 H), 7.84 (br s, 1 H), 7.69 (br s, 1 H), 7.64 (s, 1 H), 7.43 (d, *J* = 5.6 Hz, 1 H), 4.49 (dd, *J* = 4.0, 10.9 Hz, 1 H), 4.30 (dd, *J* = 6.8, 11.0 Hz, 1 H), 4.07–4.00 (m, 1 H), 3.99 (s, 3 H), 2.37–2.15 (m, 3 H), 1.96–1.86 (m, 1 H). <sup>13</sup>C NMR (126 MHz, DMSO-*d*<sub>6</sub>) δ 177.13, 166.32, 158.51, 155.15, 137.72, 131.79, 130.29, 128.46, 120.21, 115.17, 102.81, 69.26, 55.97, 52.30, 29.63, 22.90. LCMS: 316 (MH<sup>+</sup>). HRMS: calcd mass for C<sub>16</sub>H<sub>18</sub>N<sub>3</sub>O<sub>4</sub> (MH<sup>+</sup>) 316.1292; found 316.1295; difference 1.05 ppm. HPLC purity: 100%.

**(S)-7-Ethoxy-1-((5-oxopyrrololidin-2-yl)methoxy)isoquinoline-6-carboxamide (22).** This was prepared from 1-chloro-7-ethoxyisoquino-

line-6-carbonitrile<sup>37</sup> (**18**) and (*S*)-5-(hydroxymethyl)-pyrrolidin-2-one according to the general procedure for the preparation of **40**; mp 242–244 °C. <sup>1</sup>H NMR (400 MHz, DMSO-*d*<sub>6</sub>) δ 8.17 (s, 1H), 8.14 (s, 1H), 7.88 (d, *J* = 5.1 Hz, 1H), 7.78 (br s, 1H), 7.72 (br s, 1H), 7.62 (s, 1H), 7.41 (d, *J* = 5.5 Hz, 1H), 4.54–4.42 (m, 1H), 4.37–4.17 (m, 3H), 4.09–3.96 (m, 1H), 2.37–2.13 (m, 3H), 1.97–1.82 (m, 1H), 1.44 (t, *J* = 6.4 Hz, 3H). <sup>13</sup>C NMR (101 MHz, DMSO-*d*<sub>6</sub>) δ 177.09, 166.34, 158.48, 154.35, 137.66, 131.69, 130.29, 128.58, 120.25, 115.15, 103.61, 69.21, 64.35, 52.30, 29.63, 22.90, 14.33. LCMS: 330 (MH<sup>+</sup>). HRMS: calcd mass for C<sub>17</sub>H<sub>20</sub>N<sub>3</sub>O<sub>4</sub> (MH<sup>+</sup>) 330.1448; found 330.146; difference 3.65 ppm. HPLC purity: 98.29%.

(*S*)-6-Methoxy-4-((5-oxopyrrolidin-2-yl)methoxy)quinoline-7-carboxamide (**23**). This was prepared from 4-chloro-6-methoxyquinoline-7-carbonitrile<sup>37</sup> (**19**) and (*S*)-5-(hydroxymethyl)-pyrrolidin-2-one according to the general procedure for the preparation of **40**; mp 247–250 °C. <sup>1</sup>H NMR (500 MHz, DMSO-*d*<sub>6</sub>) δ 8.63 (d, *J* = 5.1 Hz, 1H), 8.21 (s, 1H), 8.16 (s, 1H), 7.84 (br s, 1H), 7.68 (br s, 1H), 7.57 (s, 1H), 7.02 (d, *J* = 5.1 Hz, 1H), 4.24 (dd, *J* = 3.4, 9.8 Hz, 1H), 4.17–4.11 (m, 1H), 4.11–4.04 (m, 1H), 3.99 (s, 3H), 2.41–2.17 (m, 3H), 1.96–1.87 (m, 1H). <sup>13</sup>C NMR (126 MHz, DMSO-*d*<sub>6</sub>) δ 177.21, 166.19, 159.39, 154.11, 149.81, 143.50, 130.73, 128.94, 122.35, 102.41, 100.67, 71.80, 56.03, 52.22, 29.62, 22.74. LCMS: 316 (MH<sup>+</sup>). HRMS: calcd mass for C<sub>16</sub>H<sub>18</sub>N<sub>3</sub>O<sub>4</sub> (MH<sup>+</sup>) 316.1292; found 316.1305; difference 4.17 ppm. HPLC purity: 95.31%.

(*R*)-7-Isopropoxy-1-((5-oxopyrrolidin-2-yl)methoxy)isoquinoline-6-carboxamide (**24**). This was prepared from **15** and (*R*)-5-(hydroxymethyl)-pyrrolidin-2-one according to the general procedure for the preparation of **40**; mp 208–210 °C. <sup>1</sup>H NMR (400 MHz, DMSO-*d*<sub>6</sub>) δ 8.19 (s, 1H), 8.09 (br s, 1H), 7.88 (d, *J* = 5.5 Hz, 1H), 7.73 (br s, 1H), 7.70 (br s, 1H), 7.64 (s, 1H), 7.41 (d, *J* = 5.9 Hz, 1H), 4.91 (spt, *J* = 6.0 Hz, 1H), 4.47 (dd, *J* = 3.5, 10.9 Hz, 1H), 4.31 (dd, *J* = 6.2, 10.9 Hz, 1H), 4.07–3.97 (m, *J* = 6.2 Hz, 1H), 2.37–2.13 (m, 3H), 1.97–1.86 (m, 1H), 1.45–1.33 (m, 6H). <sup>13</sup>C NMR (101 MHz, DMSO-*d*<sub>6</sub>) δ 177.06, 166.36, 158.45, 153.23, 137.64, 131.57, 130.93, 128.80, 120.28, 115.12, 105.05, 71.18, 69.14, 52.27, 29.68, 22.92, 21.62, 21.40. LCMS: 344 (MH<sup>+</sup>). HRMS: calcd mass for C<sub>18</sub>H<sub>22</sub>N<sub>3</sub>O<sub>4</sub> (MH<sup>+</sup>) 344.1605; found 344.1614; difference 2.54 ppm. HPLC purity: 94.75%.

(*S*)-3-Methoxy-5-((5-oxopyrrolidin-2-yl)methoxy)-2-naphthamide (**26**). Triphenylphosphine (655 mg, 2.45 mmol), 5-hydroxy-3-methoxy-2-naphthamide<sup>37</sup> (**25**, 200 mg, 0.92 mmol), and (*S*)-5-(hydroxymethyl)-pyrrolidin-2-one (170 mg, 1.4 mmol) were combined in THF (8 mL) at 20 °C. Diisopropyl azodicarboxylate (0.35 mL, 1.7 mmol) was then added, and the reaction mixture was heated at 60 °C for 20 h. The mixture was concentrated to dryness and purified by chromatography to afford 130 mg (45%) of **26** as a colorless solid; mp 198–201 °C. <sup>1</sup>H NMR (400 MHz, DMSO-*d*<sub>6</sub>) δ 8.28 (s, 1H), 8.05 (br s, 1H), 8.11–7.98 (m, 1H), 7.77 (br s, 1H), 7.59 (s, 2H), 7.52 (d, *J* = 8.2 Hz, 1H), 7.31 (t, *J* = 8.0 Hz, 1H), 7.01 (d, *J* = 7.8 Hz, 1H), 4.18–4.02 (m, 3H), 3.99 (s, 3H), 2.44–2.15 (m, 3H), 2.02–1.89 (m, 1H). <sup>13</sup>C NMR (101 MHz, DMSO-*d*<sub>6</sub>) δ 177.18, 166.33, 154.29, 152.76, 130.80, 128.36, 126.66, 125.27, 124.28, 120.74, 106.89, 100.88, 71.40, 55.72, 52.53, 29.75, 23.00. LCMS: 315 (MH<sup>+</sup>), 337 (M + Na<sup>+</sup>). HRMS: calcd mass for C<sub>17</sub>H<sub>19</sub>N<sub>2</sub>O<sub>4</sub> (MH<sup>+</sup>) 315.1339; found 315.1342; difference 0.83 ppm. HPLC purity: 97.82%.

(*R,R*)-7-(Methoxymethyl)-3,3-dimethyltetrahydro-3*H*,5*H*-pyrrolo[1,2-*c*]oxazol-5-one (**28e**). A stream of ozonized oxygen was bubbled through a solution of (*7S,7aS*)-3,3-dimethyl-7-vinyltetrahydro-3*H*,5*H*-pyrrolo[1,2-*c*]oxazol-5-one<sup>38</sup> (**28d**, 1.95 g, 10.8 mmol) in DCM (49 mL) and MeOH (16 mL) at about –78 °C for about 2 h. Dimethyl sulfide (10 mL) was added at about –78 °C, followed NaBH<sub>4</sub> (2.44 g, 64.6 mmol) at the same temperature. After about 30 min, the reaction was warmed to about 0 °C and stirred for about 2 h. Ethyl acetate was added, and the mixture was washed with water, then brine. The combined EtOAc extracts were dried over Na<sub>2</sub>SO<sub>4</sub>, filtered, and concentrated. The residue was purified by chromatography to provide 1.20 g (60%) of (*7R,7aS*)-7-(hydroxymethyl)-3,3-dimethyltetrahydro-3*H*,5*H*-pyrrolo[1,2-*c*]oxazol-5-one as a colorless oil. <sup>1</sup>H NMR (400 MHz, CDCl<sub>3</sub>) δ 4.40–4.34 (m, 1H), 3.97 (dd, 1H), 3.86 (dd, 1H), 3.72–3.62 (m, 2H), 2.94 (dd, 1H), 2.58–2.53 (m, 1H), 2.25 (d, 1H), 1.64 (s, 3H), 1.45 (s, 3H). LCMS: 186 (MH<sup>+</sup>). To a stirred solution of

the above compound (1.40 g, 7.5 mmol) in THF (40 mL) was added freshly prepared silver(I) oxide (17.48 g, 75.7 mmol), followed by iodomethane (5.37 g, 37.8 mmol). The mixture was heated at 70 °C for 16 h, then cooled to about 25 °C, filtered, and concentrated. The residue was purified by chromatography to provide 1.10 g (73%) of **28e** as a colorless oil. <sup>1</sup>H NMR (400 MHz, CDCl<sub>3</sub>) δ 4.35 (td, *J* = 6.3, 10.1 Hz, 1H), 3.95 (dd, *J* = 5.9, 8.9 Hz, 1H), 3.74–3.66 (m, 1H), 3.33 (s, 3H), 3.43–3.27 (m, 2H), 2.96 (dd, *J* = 8.4, 16.8 Hz, 1H), 2.66–2.57 (m, 1H), 2.24 (dd, *J* = 1.5, 16.8 Hz, 1H), 1.65 (s, 3H), 1.48 (s, 3H). LCMS: 200 (MH<sup>+</sup>).

(*R,R*)-5-(Hydroxymethyl)-4-methylpyrrolidin-2-one (**29a**). This compound was prepared from **28a** according to the general procedure for the preparation of **35e**. <sup>1</sup>H NMR (400 MHz, CD<sub>3</sub>OD) δ 3.53–3.71 (m, 3H), 2.57–2.74 (m, 1H), 2.36 (dd, *J* = 16.43, 8.61 Hz, 1H), 2.10 (dd, *J* = 16.43, 9.00 Hz, 1H), 1.11 (d, *J* = 7.04 Hz, 3H). LCMS: 130 (MH<sup>+</sup>).

(*R,R*)-4-Ethyl-5-(hydroxymethyl)pyrrolidin-2-one (**29b**). This compound was prepared from **28b** according to the general procedure for the preparation of **35e**. <sup>1</sup>H NMR (400 MHz, DMSO-*d*<sub>6</sub>) δ 7.45 (br s, 1H), 3.47–3.35 (m, 3H), 2.35–2.20 (m, 1H), 2.06 (dd, *J* = 7.8, 16.0 Hz, 1H), 1.92 (dd, *J* = 11.3, 16.4 Hz, 1H), 1.59–1.45 (m, 1H), 1.42–1.28 (m, 1H), 0.87 (t, *J* = 7.4 Hz, 3H). LCMS: 144 (MH<sup>+</sup>).

(*R,R*)-5-(Hydroxymethyl)-4-propylpyrrolidin-2-one (**29c**). This compound was prepared from **28c** according to the general procedure for the preparation of **35e**. <sup>1</sup>H NMR (400 MHz, DMSO-*d*<sub>6</sub>) δ 7.46 (br s, 1H), 4.63 (t, 1H), 3.44–3.36 (m, 3H), 2.37–2.31 (m, 1H), 2.07–2.01 (dd, 1H), 1.95–1.89 (dd, 1H), 1.48–1.41 (m, 1H), 1.39–1.20 (m, 3H), 0.86 (t, H). LCMS: 158 (MH<sup>+</sup>).

(*R,R*)-5-(Hydroxymethyl)-4-(methoxymethyl)pyrrolidin-2-one (**29e**). This compound was prepared from **28e** according to the general procedure for the preparation of **35e**. <sup>1</sup>H NMR (400 MHz, DMSO-*d*<sub>6</sub>) δ 3.49–3.34 (m, 5H), 3.32 (s, 3H), 3.23 (s, 3H), 2.73–2.60 (m, 1H), 2.09–1.95 (m, 2H). LCMS: 160 (MH<sup>+</sup>).

7-Methoxy-1-((2S,3R)-3-methyl-5-oxopyrrolidin-2-yl)methoxy)-isoquinoline-6-carboxamide (**30**). This was prepared from **17** and (*R,R*)-5-(hydroxymethyl)-4-methylpyrrolidin-2-one (**29a**) according to the general procedure for the preparation of **40**; mp 224–226 °C. <sup>1</sup>H NMR (400 MHz, DMSO-*d*<sub>6</sub>) δ 8.17 (s, 1H), 8.00 (br s, 1H), 7.91 (d, *J* = 5.5 Hz, 1H), 7.83 (br s, 1H), 7.69 (br s, 1H), 7.58 (s, 1H), 7.43 (d, *J* = 5.9 Hz, 1H), 4.48 (dd, *J* = 3.9, 10.5 Hz, 1H), 4.43 (dd, *J* = 5.5, 11.3 Hz, 1H), 3.98 (s, 3H), 3.96–3.90 (m, 1H), 2.78–2.64 (m, 1H), 2.32 (dd, *J* = 9.0, 16.4 Hz, 1H), 2.09 (dd, *J* = 9.8, 16.4 Hz, 1H), 1.09 (d, *J* = 6.6 Hz, 3H). <sup>13</sup>C NMR (126 MHz, DMSO-*d*<sub>6</sub>) δ 176.82, 166.34, 158.43, 155.21, 137.69, 131.80, 130.38, 128.51, 120.21, 115.21, 102.70, 66.11, 55.97, 55.18, 38.22, 31.13, 14.61. LCMS: 330 (MH<sup>+</sup>), 352 (MNa<sup>+</sup>). HRMS: calcd mass for C<sub>17</sub>H<sub>20</sub>N<sub>3</sub>O<sub>4</sub> (MH<sup>+</sup>) 330.1448; found 330.1456; difference 2.35 ppm. HPLC purity: 99.75%.

7-Methoxy-1-((2S,3R)-3-ethyl-5-oxopyrrolidin-2-yl)methoxy)-isoquinoline-6-carboxamide (**31**). This was prepared from **17** and (*R,R*)-4-ethyl-5-(hydroxymethyl)pyrrolidin-2-one (**29b**) according to the general procedure for the preparation of **40**; mp 243–244 °C. <sup>1</sup>H NMR (500 MHz, DMSO-*d*<sub>6</sub>) δ 8.16 (s, 1H), 8.04 (br s, 1H), 7.90 (d, *J* = 5.9 Hz, 1H), 7.84 (br s, 1H), 7.71 (br s, 1H), 7.56 (s, 1H), 7.42 (d, *J* = 5.9 Hz, 1H), 4.48–4.41 (m, 2H), 3.97 (s, 3H), 3.96–3.92 (m, 1H), 2.27 (dd, *J* = 8.1, 17.1 Hz, 1H), 2.14 (dd, *J* = 10.8, 16.4 Hz, 1H), 1.59 (quind, *J* = 6.8, 13.5 Hz, 1H), 1.43–1.29 (m, 1H), 0.92 (t, *J* = 7.2 Hz, 3H). <sup>13</sup>C NMR (126 MHz, DMSO-*d*<sub>6</sub>) δ 176.71, 166.31, 158.43, 155.19, 137.83, 131.76, 130.29, 128.52, 120.18, 115.16, 102.65, 65.97, 55.93, 54.62, 38.83, 36.04, 22.42, 12.66. LCMS: 344 (MH<sup>+</sup>). HRMS: calcd mass for C<sub>18</sub>H<sub>22</sub>N<sub>3</sub>O<sub>4</sub> (MH<sup>+</sup>) 344.1605; found 344.1611; difference 1.78 ppm. HPLC purity: 99.13%.

7-Methoxy-1-((2S,3R)-5-oxo-3-propylpyrrolidin-2-yl)methoxy)-isoquinoline-6-carboxamide (**32**). This was prepared from **17** and (*R,R*)-5-(hydroxymethyl)-4-propylpyrrolidin-2-one (**29c**) according to the general procedure for the preparation of **40**; mp 193–195 °C. <sup>1</sup>H NMR (500 MHz, DMSO-*d*<sub>6</sub>) δ 8.17 (s, 1H), 8.03 (br s, 1H), 7.91 (d, *J* = 5.9 Hz, 1H), 7.84 (br s, 1H), 7.70 (br s, 1H), 7.57 (s, 1H), 7.43 (d, *J* = 5.9 Hz, 1H), 4.47–4.41 (m, 2H), 3.98 (s, 3H), 3.94 (td, *J* = 4.2, 7.9 Hz, 1H), 2.65–2.54 (m, 1H), 2.26 (dd, *J* = 8.3, 16.4 Hz, 1H), 2.15 (dd, *J* = 10.8, 16.6 Hz, 1H), 1.58–1.47 (m, 1H), 1.44–1.25 (m, 3H), 0.88 (t, *J* = 7.0

Hz, 3H).  $^{13}\text{C}$  NMR (126 MHz, DMSO- $d_6$ )  $\delta$  176.72, 166.29, 158.45, 155.18, 137.82, 131.77, 130.31, 128.51, 120.18, 115.16, 102.65, 66.02, 55.92, 54.70, 36.75, 36.18, 31.61, 20.96, 14.06. LCMS: 358 ( $\text{MH}^+$ ). HRMS: calcd mass for  $\text{C}_{19}\text{H}_{24}\text{N}_3\text{O}_4$  ( $\text{MH}^+$ ) 358.1761; found 358.1762; difference 0.32 ppm. HPLC purity: 95.10%.

**7-Methoxy-1-((2S,3R)-3-(methoxymethyl)-5-oxopyrrolidin-2-yl)methoxy)isoquinoline-6-carboxamide (33).** This was prepared from 17 and (4R,SS)-5-(hydroxymethyl)-4-(methoxymethyl)pyrrolidin-2-one (29e) according to the general procedure for the preparation of 40; mp 182–184 °C.  $^1\text{H}$  NMR (500 MHz, DMSO- $d_6$ )  $\delta$  8.17 (s, 1H), 8.09 (br s, 1H), 8.10–8.08 (m, 1H), 7.91 (d,  $J$  = 5.9 Hz, 1H), 7.84 (br s, 1H), 7.69 (br s, 1H), 7.58 (s, 1H), 7.43 (d,  $J$  = 5.9 Hz, 1H), 4.49 (dd,  $J$  = 3.7, 11.0 Hz, 1H), 4.45 (dd,  $J$  = 5.6, 11.2 Hz, 1H), 4.04–3.99 (m, 1H), 3.98 (s, 3H), 3.52–3.42 (m, 2H), 3.24 (s, 3H), 2.91 (qd,  $J$  = 8.3, 16.7 Hz, 1H), 2.25 (dd,  $J$  = 9.0, 16.4 Hz, 1H), 2.19 (dd,  $J$  = 10.3, 16.9 Hz, 1H).  $^{13}\text{C}$  NMR (126 MHz, DMSO- $d_6$ )  $\delta$  176.19, 166.30, 158.40, 155.17, 137.81, 131.77, 130.31, 128.49, 120.19, 115.19, 102.71, 71.39, 65.97, 58.20, 55.94, 53.78, 36.34, 33.55. LCMS: 360 ( $\text{MH}^+$ ). HRMS: calcd mass for  $\text{C}_{18}\text{H}_{22}\text{N}_3\text{O}_5$  ( $\text{MH}^+$ ) 360.1554; found 360.156; difference 1.74 ppm. HPLC purity: 93.70%.

**(6S,7R,7aS)-3,3,6,7-Tetramethyltetrahydro-3H,5H-pyrrolo[1,2-c]oxazol-5-one (34a).** This compound was prepared from 28a and  $\text{CH}_3\text{I}$  according to the general procedure for the preparation of 34e.  $^1\text{H}$  NMR (400 MHz,  $\text{CDCl}_3$ )  $\delta$  4.24 (td,  $J$  = 6.1, 8.8 Hz, 1H), 3.95–3.86 (m, 1H), 3.74 (t,  $J$  = 9.0 Hz, 1H), 2.50 (dd,  $J$  = 6.5, 13.1 Hz, 1H), 2.12 (dt,  $J$  = 2.8, 6.9 Hz, 1H), 1.62 (s, 3H), 1.49–1.45 (s, 3H), 1.08 (d,  $J$  = 7.0 Hz, 3H), 0.87 (d,  $J$  = 7.5 Hz, 3H).

**(6R,7R,7aS)-3,3,6,7-Tetramethyltetrahydro-3H,5H-pyrrolo[1,2-c]oxazol-5-one (34b).** This compound was prepared from 28a and  $\text{CH}_3\text{I}$  according to the general procedure for the preparation of 34e.  $^1\text{H}$  NMR (400 MHz,  $\text{CDCl}_3$ )  $\delta$  4.33 (td,  $J$  = 6.5, 9.7 Hz, 1H), 3.95–3.86 (m, 1H), 3.70–3.64 (m, 1H), 2.97 (quin,  $J$  = 7.3 Hz, 1H), 2.28 (dq,  $J$  = 2.8, 7.4 Hz, 1H), 1.66 (s, 3H), 1.49–1.45 (s, 3H), 1.30 (d,  $J$  = 7.5 Hz, 3H), 1.04 (d,  $J$  = 7.5 Hz, 3H).

**(6S,7S,7aS)-6-Fluoro-3,3,7-trimethyltetrahydro-3H,5H-pyrrolo[1,2-c]oxazol-5-one (34c).** This compound was prepared from 28a and NFSI according to the general procedure for the preparation of 34e.  $^1\text{H}$  NMR (400 MHz,  $\text{CDCl}_3$ )  $\delta$  5.25 (dd,  $J$  = 51.90, 7.41 Hz, 1H), 3.95–4.10 (m, 2H), 3.71–3.82 (m, 1H), 2.86–3.03 (m, 1H), 1.68 (s, 3H), 1.49 (s, 3H), 1.01 (dd,  $J$  = 7.02, 2.34 Hz, 3H).  $^{19}\text{F}$  NMR (376 MHz,  $\text{CDCl}_3$ )  $\delta$  –202.08.

**(6R,7S,7aS)-6-Fluoro-3,3,7-trimethyltetrahydro-3H,5H-pyrrolo[1,2-c]oxazol-5-one (34d).** This compound was prepared from 28a and NFSI according to the general procedure for the preparation of 34e.  $^1\text{H}$  NMR (400 MHz,  $\text{CDCl}_3$ )  $\delta$  4.58–4.77 (m, 1H), 4.54 (ddt,  $J$  = 9.51, 6.07, 6.07, 1.17 Hz, 1H), 3.96 (dd,  $J$  = 8.68, 6.15 Hz, 1H), 3.68 (dd,  $J$  = 9.56, 8.78 Hz, 1H), 2.53–2.73 (m, 1H), 1.66 (s, 3H), 1.53 (s, 3H), 1.05 (d,  $J$  = 8.20 Hz, 3H).  $^{19}\text{F}$  NMR (376 MHz,  $\text{CDCl}_3$ )  $\delta$  –184.92.

**General Procedure for Preparation of Bicyclic Lactams 34a–34f: (6S,7S,7aS)-7-Ethyl-6-fluoro-3,3-dimethyltetrahydro-3H,5H-pyrrolo[1,2-c]oxazol-5-one (34e).** A solution of 28b (1.03 g, 5.6 mmol) in THF (20 mL) was cooled to –78 °C and treated with LDA (2.0 M, 4.68 mL, 8.4 mmol). The mixture was kept at –78 °C for 25 min before being treated with NFSI (2.28 g, 7.0 mmol) in THF (5 mL). After stirring at –78 °C for another 5 min, the mixture was warmed to 25 °C for 1 h. Ethyl acetate and water were added, and the mixture was concentrated under reduced pressure to remove the THF present. The mixture was extracted twice with ethyl acetate, and the combined extracts were dried over  $\text{Na}_2\text{SO}_4$ , filtered, and concentrated. The residue was purified by chromatography to provide 265 mg (23%) of 34e as a colorless solid and 509 mg (45%) of 34f as a colorless oil.

**(6S,7S,7aS)-7-Ethyl-6-fluoro-3,3-dimethyltetrahydro-3H,5H-pyrrolo[1,2-c]oxazol-5-one (34e).**  $^1\text{H}$  NMR (400 MHz,  $\text{CDCl}_3$ )  $\delta$  5.22 (dd,  $J$  = 7.4, 51.9 Hz, 1H), 4.09–3.99 (m, 2H), 3.76–3.66 (m, 1H), 2.73–2.63 (m, 1H), 1.67 (s, 3H), 1.76–1.63 (m, 1H), 1.48 (s, 3H), 1.34 (tt,  $J$  = 7.4, 15.0 Hz, 1H), 0.96 (t,  $J$  = 7.2 Hz, 3H).  $^{19}\text{F}$  NMR (376 MHz,  $\text{CDCl}_3$ )  $\delta$  –199.61.

**(6R,7S,7aS)-7-Ethyl-6-fluoro-3,3-dimethyltetrahydro-3H,5H-pyrrolo[1,2-c]oxazol-5-one (34f).**  $^1\text{H}$  NMR (400 MHz,  $\text{CDCl}_3$ )  $\delta$  4.77 (dd,  $J$  = 2.0, 51.1 Hz, 1H), 4.48 (td,  $J$  = 6.2, 10.1 Hz, 1H), 3.97 (dd,  $J$  = 5.9, 8.6 Hz, 1H), 3.62 (dd,  $J$  = 8.6, 10.1 Hz, 1H), 2.47–2.32 (m, 1H),

1.65 (s, 3H), 1.52 (s, 3H), 1.60–1.47 (m, 1H), 1.46–1.33 (m, 1H).  $^{19}\text{F}$  NMR (376 MHz,  $\text{CD}_3\text{CN}$ )  $\delta$  –185.41.

**(4R,5S)-5-(Hydroxymethyl)-3,4-dimethylpyrrolidin-2-one (35a); 35b, approximately 1:2 ratio of 35a:35b.** This compound was prepared from a 1:2 mixture of 34a and 34b according to the general procedure for the preparation of 35e.  $^1\text{H}$  NMR (400 MHz,  $\text{CD}_3\text{OD}$ )  $\delta$  3.75–3.50 (m, 3H), 2.70–2.58 (m, 1H), 2.29–2.15 (m, 1H), 1.21–1.05 (overlapping d, 6H).

**(3S,4S,5S)-3-Fluoro-5-(hydroxymethyl)-4-methylpyrrolidin-2-one (35c).** This compound was prepared from 34c according to the general procedure for the preparation of 35e.  $^1\text{H}$  NMR (400 MHz,  $\text{CDCl}_3$ )  $\delta$  6.63 (br s, 1H) 4.86 (br, dd,  $J$  = 53.00, 6.80 Hz, 1H) 3.72–3.83 (m, 2H) 3.60–3.68 (m, 1H) 2.67–2.80 (m, 1H) 1.96 (br s, 1H) 1.10 (dd,  $J$  = 7.41, 1.56 Hz, 3H).  $^{19}\text{F}$  NMR (376 MHz,  $\text{CDCl}_3$ )  $\delta$  –201.74. LCMS: 148 ( $\text{MH}^+$ ).

**(3R,4S,5S)-3-Fluoro-5-(hydroxymethyl)-4-methylpyrrolidin-2-one (35d).** This compound was prepared from 34d according to the general procedure for the preparation of 35e.  $^1\text{H}$  NMR (400 MHz,  $\text{CDCl}_3$ )  $\delta$  6.94 (br s, 1H) 4.94 (dd,  $J$  = 54.00, 9.00 Hz, 1H) 3.66–3.77 (m, 2H) 3.60–3.66 (m, 1H) 2.93 (t,  $J$  = 5.46 Hz, 1H) 2.61–2.81 (m, 1H) 1.29 (d,  $J$  = 7.02 Hz, 3H).  $^{19}\text{F}$  NMR (376 MHz,  $\text{CDCl}_3$ )  $\delta$  –194.85. LCMS: 148 ( $\text{MH}^+$ ).

**General Procedure for Preparation of Lactam Alcohols 29a–29e, 35a–35f, 43a–43b, 49: (3S,4S,5S)-4-Ethyl-3-fluoro-5-(hydroxymethyl)pyrrolidin-2-one (35e).** To a stirred solution of compound 34e (500 mg, 2.48 mmol) in 9 mL of acetonitrile and 1 mL of water was added 4-toluenesulfonic acid (27 mg, 0.16 mmol). The reaction mixture was heated at 90 °C for 2 h, then the mixture was cooled to 25 °C, concentrated, and the residue purified by chromatography to provide 388 mg (97%) of 35e as a colorless solid.  $^1\text{H}$  NMR (400 MHz,  $\text{CDCl}_3$ )  $\delta$  6.52 (br s, 1H), 4.80 (dd,  $J$  = 5.9, 52.7 Hz, 2H), 3.84–3.73 (m, 2H), 3.67–3.56 (m, 1H), 2.51–2.38 (m, 1H), 1.73–1.60 (m, 1H), 1.56–1.46 (m, 1H), 1.07 (t,  $J$  = 7.2 Hz, 3H).  $^{19}\text{F}$  NMR (376 MHz,  $\text{CDCl}_3$ )  $\delta$  –198.72. LCMS: 162 ( $\text{MH}^+$ ).

**(3R,4S,5S)-4-Ethyl-3-fluoro-5-(hydroxymethyl)pyrrolidin-2-one (35f).** This compound was prepared from 34f according to the general procedure for the preparation of 35e.  $^1\text{H}$  NMR (400 MHz, DMSO- $d_6$ )  $\delta$  8.05 (br s, 1H), 4.88 (dd, 1H), 3.48–3.46 (m, 1H), 3.41–3.38 (m, 2H), 2.32–2.23 (m, 1H), 1.62–1.55 (m, 2H), 0.95 (t, 3H). LCMS: 162 ( $\text{MH}^+$ ).

**1-((2S,3R,4S)-3,4-Dimethyl-5-oxopyrrolidin-2-yl)methoxy)-7-methoxyisoquinoline-6-carboxamide (36).** This was prepared from 17 and (4R,SS)-5-(hydroxymethyl)-3,4-dimethylpyrrolidin-2-one (approximately 1:2 ratio of 35a:35b) according to the general procedure for the preparation of 40 followed by SFC separation from 37; mp 250–253 °C.  $^1\text{H}$  NMR (500 MHz, DMSO- $d_6$ )  $\delta$  8.17 (s, 1H), 8.19–8.16 (m, 1H), 7.90 (d,  $J$  = 5.9 Hz, 1H), 7.85 (br s, 1H), 7.70 (br s, 1H), 7.62 (s, 2H), 7.42 (d,  $J$  = 5.9 Hz, 1H), 4.47 (dd,  $J$  = 4.2, 10.8 Hz, 1H), 4.39 (dd,  $J$  = 5.6, 10.8 Hz, 1H), 4.00 (s, 3H), 3.90–3.84 (m, 1H), 2.01–1.95 (m, 1H), 1.80–1.74 (m, 1H), 1.11–1.05 (m, 1H), 0.59 (q,  $J$  = 3.9 Hz, 1H).  $^{13}\text{C}$  NMR (126 MHz, DMSO- $d_6$ )  $\delta$  176.95, 166.32, 158.52, 155.17, 137.77, 131.78, 130.25, 128.52, 120.27, 115.17, 102.72, 69.04, 55.97, 53.66, 18.89, 16.77, 11.22. LCMS: 328 ( $\text{MH}^+$ ). HRMS: calcd mass for  $\text{C}_{17}\text{H}_{17}\text{N}_3\text{NaO}_4$  ( $\text{MH}^+$ ) 350.1111; found 350.1128; difference 4.70 ppm. Analysis: Calcd for  $\text{C}_{17}\text{H}_{17}\text{N}_3\text{O}_4$ : C, 62.38%; H, 5.23%; N, 12.84%. Found: C, 62.08%; H, 5.05%; N, 12.75%.

**1-((2S,3R,4R)-3,4-Dimethyl-5-oxopyrrolidin-2-yl)methoxy)-7-methoxyisoquinoline-6-carboxamide (37).** This was prepared from 17 and (4R,SS)-5-(hydroxymethyl)-3,4-dimethylpyrrolidin-2-one (approximately 1:2 ratio of 35a:35b) according to the general procedure for the preparation of 40 followed by SFC separation from 36; mp 242–244 °C.  $^1\text{H}$  NMR (400 MHz, DMSO- $d_6$ )  $\delta$  8.16 (s, 1H), 8.05 (br s, 1H), 7.91 (d,  $J$  = 5.9 Hz, 1H), 7.82 (br s, 1H), 7.69 (br s, 1H), 7.56 (s, 1H), 7.43 (d,  $J$  = 5.9 Hz, 1H), 4.48 (dd,  $J$  = 3.5, 11.3 Hz, 1H), 4.42 (dd,  $J$  = 5.9, 10.9 Hz, 1H), 3.97 (s, 3H), 3.86 (br s, 1H), 2.22 (s, 2H), 1.12 (d,  $J$  = 5.9 Hz, 3H), 1.06 (d,  $J$  = 5.9 Hz, 3H).  $^{13}\text{C}$  NMR (101 MHz,  $\text{CDCl}_3$ )  $\delta$  180.66, 166.00, 158.57, 155.49, 138.14, 132.25, 125.66, 121.60, 115.86, 103.04, 65.86, 56.28, 54.52, 42.69, 40.27, 14.21, 13.66. LCMS: 344 ( $\text{MH}^+$ ). HRMS: calcd mass for  $\text{C}_{18}\text{H}_{22}\text{N}_3\text{O}_4$  ( $\text{MH}^+$ ) 344.1605; found 344.1604; difference –0.22 ppm. HPLC purity: 99.78%.

**1-(((2S,3S,4S)-4-Fluoro-3-methyl-5-oxopyrrolidin-2-yl)methoxy)-7-methoxyisoquinoline-6-carboxamide (38).** This was prepared from **17** and (*3S,4S,5S*)-3-fluoro-5-(hydroxymethyl)-4-methylpyrrolidin-2-one (**35c**) according to the general procedure for the preparation of **40**; mp 233–234 °C. <sup>1</sup>H NMR (500 MHz, DMSO-*d*<sub>6</sub>) δ 8.76 (br s, 1H), 8.16 (s, 1H), 7.90 (d, *J* = 5.6 Hz, 1H), 7.84 (br s, 1H), 7.71 (s, 1H), 7.69 (br s, 1H), 7.43 (d, *J* = 5.9 Hz, 1H), 4.93 (dd, *J* = 6.6, 53.3 Hz, 1H), 4.57 (dd, *J* = 4.0, 11.1 Hz, 1H), 4.29 (dd, *J* = 6.5, 11.1 Hz, 1H), 4.08–4.02 (m, 1H), 3.97 (s, 3H), 2.94–2.79 (m, 1H), 1.09 (dd, *J* = 1.5, 7.3 Hz, 3H). <sup>13</sup>C NMR (126 MHz, DMSO-*d*<sub>6</sub>) δ 171.62 (d, *J* = 19.4 Hz, 1C), 166.87, 158.87, 155.67, 138.23, 132.29, 130.81, 128.90, 120.79, 115.77, 103.58 (d, *J* = 2.5 Hz, 1C), 91.27 (d, *J* = 182.6 Hz, 1C), 66.49, 56.49, 53.97, 35.26 (d, *J* = 18.5 Hz, 1C), 8.10 (d, *J* = 10.1 Hz, 1C). <sup>19</sup>F NMR (H decoupled, 376 MHz, DMSO-*d*<sub>6</sub>) δ –200.82. LCMS: 348 (MH<sup>+</sup>). HRMS: calcd mass for C<sub>17</sub>H<sub>19</sub>FN<sub>3</sub>O<sub>4</sub> (MH<sup>+</sup>) 348.1354; found 348.1364; difference 2.75 ppm. HPLC: 99.38%.

**1-((2S,3S,4R)-4-Fluoro-3-methyl-5-oxopyrrolidin-2-yl)methoxy)-7-methoxyisoquinoline-6-carboxamide (39).** This was prepared from **17** and (*3R,4S,5S*)-3-fluoro-5-(hydroxymethyl)-4-methylpyrrolidin-2-one (**35d**) according to the general procedure for the preparation of **40**; mp 292–294 °C. <sup>1</sup>H NMR (400 MHz, DMSO-*d*<sub>6</sub>) δ 8.62 (s, 1H), 8.18 (s, 1H), 7.92 (d, *J* = 5.9 Hz, 1H), 7.83 (br s, 1H), 7.69 (br s, 1H), 7.49 (s, 1H), 7.45 (d, *J* = 5.9 Hz, 1H), 5.06 (dd, *J* = 8.6, 53.9 Hz, 1H), 4.46 (d, *J* = 3.9 Hz, 2H), 4.05–3.99 (m, 1H), 2.85–2.64 (m, 1H), 1.20 (d, *J* = 7.0 Hz, 3H). <sup>13</sup>C NMR (101 MHz, DMSO-*d*<sub>6</sub>) δ 171.06 (d, *J* = 19.8 Hz, 1C), 166.01, 157.88, 155.02, 137.53, 131.61, 130.21, 128.36, 119.78, 115.21, 102.12, 93.41 (d, *J* = 183.4 Hz, 1C), 65.08, 55.65, 51.81 (d, *J* = 8.8 Hz, 1C), 38.16 (d, *J* = 18.3 Hz, 1C), 11.86. <sup>19</sup>F NMR (376 MHz, DMSO-*d*<sub>6</sub>) δ –194.13. LCMS: 348 (MH<sup>+</sup>). HRMS: calcd mass for C<sub>17</sub>H<sub>19</sub>FN<sub>3</sub>O<sub>4</sub> (MH<sup>+</sup>) 348.1354; found 348.1356; difference –0.5 ppm. HPLC: 90.36%.

**General Procedure for the Synthesis of Targets 20–24, 30–33, 36–41, 44, 45, and 50: 1-((2S,3S,4S)-3-Ethyl-4-fluoro-5-oxopyrrolidin-2-yl)methoxy)-7-methoxyisoquinoline-6-carboxamide (40).** A mixture of **35e** (387 mg, 2.40 mmol) and **17** (477 mg, 2.18 mmol) in DMF (12 mL) was treated with KHMDS (1 M in THF, 4.8 mL) at –10 °C. Upon completion of the KHMDS addition, the cooling bath was removed and the mixture was stirred at 20 °C for 30 min. The reaction mixture was then poured into a mixture of 10% (w/v) NaH<sub>2</sub>PO<sub>4</sub> and EtOAc with vigorous stirring. The EtOAc was separated, washed with water, brine, dried over Na<sub>2</sub>SO<sub>4</sub>, filtered, and concentrated. The residue was concentrated again with heptane to remove DMF before being purified by chromatography to afford 631 mg (84%) of 1-((2S,3S,4S)-3-ethyl-4-fluoro-5-oxopyrrolidin-2-yl)methoxy)-7-methoxyisoquinoline-6-carbonitrile as a white solid. <sup>1</sup>H NMR (400 MHz, CDCl<sub>3</sub>) δ = 8.03 (s, 1H), 7.94 (d, *J* = 5.5 Hz, 1H), 7.66 (s, 1H), 7.20 (d, *J* = 5.9 Hz, 1H), 6.74 (br s, 1H), 4.91 (dd, *J* = 5.9, 52.7 Hz, 1H), 4.78 (dd, *J* = 3.1, 11.7 Hz, 1H), 4.43 (dd, *J* = 6.2, 11.7 Hz, 1H), 4.22–4.15 (m, 1H), 4.05 (s, 3H), 2.70–2.50 (m, 1H), 1.92–1.79 (m, 1H), 1.75–1.64 (m, 1H), 1.14 (t, *J* = 7.4 Hz, 3H). <sup>19</sup>F NMR (376 MHz, CDCl<sub>3</sub>) δ = –199.18. LCMS: 344 (MH<sup>+</sup>).

A mixture of the above nitrile (629 mg, 1.83 mmol) and K<sub>2</sub>CO<sub>3</sub> (1.03 g, 7.3 mmol) in DMSO (10 mL) was treated with H<sub>2</sub>O<sub>2</sub> (30%, 1.1 mL, 18.0 mmol) added dropwise at 20 °C. The mixture was stirred for 2 h before Me<sub>2</sub>S (1.5 mL, 20 mmol) was added to scavenge residual H<sub>2</sub>O<sub>2</sub>. Stirring was continued for 30 min before the reaction was filtered through Celite. The filter was washed with DCM and EtOAc, and the filtrate was concentrated under high vacuum to remove DMSO. The residue was purified by chromatography to afford 597 mg (97%) of **40** as a white solid; mp 225–226 °C. <sup>1</sup>H NMR (500 MHz, DMSO-*d*<sub>6</sub>) δ 8.86 (br s, 1H), 8.16 (s, 1H), 7.90 (d, *J* = 5.9 Hz, 1H), 7.84 (br s, 1H), 7.74 (s, 1H), 7.69 (br s, 1H), 7.42 (d, *J* = 5.9 Hz, 1H), 4.90 (dd, *J* = 9.0, 54.3 Hz, 1H), 4.54 (dd, *J* = 3.7, 11.2 Hz, 1H), 4.26 (dd, *J* = 6.2, 11.1 Hz, 1H), 4.13–4.05 (m, 1H), 3.97 (s, 3H), 2.69–2.53 (m, 1H), 1.68–1.52 (m, 2H), 1.02 (t, *J* = 7.5 Hz, 3H). <sup>13</sup>C NMR (126 MHz, DMSO-*d*<sub>6</sub>) δ 171.02 (d, *J* = 18.5 Hz, 1C), 166.36, 158.41, 155.13, 137.72, 131.76, 130.27, 128.37, 120.28, 115.21, 103.15 (d, *J* = 3.4 Hz, 1C), 89.98 (d, *J* = 180.1 Hz, 1C), 66.26, 55.97, 54.05, 42.19 (d, *J* = 19.4 Hz, 1C), 16.38 (d, *J* = 7.6 Hz, 1C), 12.13. <sup>19</sup>F NMR (H decoupled, 376 MHz, DMSO-*d*<sub>6</sub>) δ –199.26. LCMS: 362 (MH<sup>+</sup>). HRMS: calcd mass for C<sub>18</sub>H<sub>21</sub>FN<sub>3</sub>O<sub>4</sub>

(MH<sup>+</sup>) 362.1511; found 362.1518; difference 2.15 ppm. Analysis: Calcd for C<sub>18</sub>H<sub>20</sub>FN<sub>3</sub>O<sub>4</sub>: C, 59.83%; H, 5.58%; N, 11.63%. Found: C, 59.94%; H, 5.51%; N, 11.63%.

**1-((2S,3S,4R)-3-Ethyl-4-fluoro-5-oxopyrrolidin-2-yl)methoxy)-7-methoxyisoquinoline-6-carboxamide (41).** This was prepared from **17** and (*3R,4S,5S*)-4-ethyl-3-fluoro-5-(hydroxymethyl)pyrrolidin-2-one (**35f**) according to the general procedure for the preparation of **40**; mp 285–286 °C. <sup>1</sup>H NMR (500 MHz, DMSO-*d*<sub>6</sub>) δ 8.64 (br s, 1H), 8.18 (s, 1H), 7.91 (d, *J* = 5.9 Hz, 1H), 7.84 (br s, 1H), 7.71 (br s, 1H), 7.48 (s, 1H), 7.45 (d, *J* = 5.9 Hz, 1H), 5.13 (dd, *J* = 8.6, 54.0 Hz, 1H), 4.48–4.39 (m, 2H), 4.09–4.03 (m, 1H), 3.98 (s, 3H), 2.62–2.51 (m, 1H), 1.69–1.54 (m, 2H), 1.01 (t, *J* = 7.3 Hz, 3H). <sup>13</sup>C NMR (126 MHz, DMSO-*d*<sub>6</sub>) δ 171.45 (d, *J* = 20.2 Hz, 1C), 166.25, 158.09, 155.25, 137.77, 131.83, 130.38, 128.62, 120.02, 115.45, 102.37, 93.01 (d, *J* = 182.6 Hz, 1C), 65.35, 55.89, 51.39 (d, *J* = 8.4 Hz, 1C), 45.41 (d, *J* = 16.8 Hz, 1C), 20.70, 12.23. <sup>19</sup>F NMR (H decoupled, 376 MHz, DMSO-*d*<sub>6</sub>) δ –189.57. LCMS: 362 (MH<sup>+</sup>). HRMS: calcd mass for C<sub>18</sub>H<sub>20</sub>FN<sub>3</sub>NaO<sub>4</sub> (M + Na<sup>+</sup>) 384.133; found 384.1349; difference 4.95 ppm. HPLC: 99.16%.

**(1R,4S,5S)-4-(Hydroxymethyl)-3-azabicyclo[3.1.0]hexan-2-one (43a).** This compound was prepared from **42a** according to the general procedure for the preparation of **35e**. <sup>1</sup>H NMR (400 MHz, CD<sub>3</sub>OD) δ 3.47–3.61 (m, 3H), 1.97 (ddd, *J* = 7.80, 5.85, 4.29 Hz, 1H), 1.75–1.86 (m, 1H), 1.19 (td, *J* = 8.10, 4.49 Hz, 1H), 0.59–0.68 (m, 1H). LCMS: 128 (MH<sup>+</sup>).

**(1R,4S,5S,6S)-4-(Hydroxymethyl)-6-methyl-3-azabicyclo[3.1.0]-hexan-2-one (43b).** This compound was prepared from **42b** according to the general procedure for the preparation of **35e**. <sup>1</sup>H NMR (400 MHz, CD<sub>3</sub>OD) δ 3.56–3.43 (m, 3H), 1.71 (dd, *J* = 3.5, 5.9 Hz, 1H), 1.57 (td, *J* = 2.2, 5.7 Hz, 1H), 1.13 (d, *J* = 5.9 Hz, 3H), 1.02 (tdd, *J* = 3.0, 5.9, 8.8 Hz, 1H). LCMS: 142 (MH<sup>+</sup>).

**7-Methoxy-1-(((1S,2S,5R)-4-oxo-3-azabicyclo[3.1.0]hexan-2-yl)methoxy)-isoquinoline-6-carboxamide (44).** This was prepared from **17** and (*1R,4S,5S*)-4-(hydroxymethyl)-3-azabicyclo[3.1.0]hexan-2-one (**43a**) according to the general procedure for the preparation of **40**; mp 250–253 °C. <sup>1</sup>H NMR (500 MHz, DMSO-*d*<sub>6</sub>) δ 8.17 (s, 1H), 7.90 (d, *J* = 5.9 Hz, 1H), 7.85 (br s, 1H), 7.70 (br s, 1H), 7.62 (s, 2H), 7.42 (d, *J* = 5.9 Hz, 1H), 4.47 (dd, *J* = 4.2, 10.8 Hz, 1H), 4.39 (dd, *J* = 5.6, 10.8 Hz, 1H), 4.00 (s, 3H), 3.90–3.84 (m, 1H), 2.01–1.95 (m, 1H), 1.80–1.74 (m, 1H), 1.11–1.05 (m, 1H), 0.59 (q, *J* = 3.9 Hz, 1H). <sup>13</sup>C NMR (126 MHz, DMSO-*d*<sub>6</sub>) δ 176.95, 166.32, 158.52, 155.17, 137.77, 131.78, 130.25, 128.52, 120.27, 115.17, 102.72, 69.04, 55.97, 53.66, 18.89, 16.77, 11.22. LCMS: 328 (MH<sup>+</sup>). HRMS: calcd mass for C<sub>17</sub>H<sub>17</sub>N<sub>3</sub>NaO<sub>4</sub> (MNa<sup>+</sup>) 350.1111; found 350.1128; difference 4.70 ppm. Analysis: Calcd for C<sub>17</sub>H<sub>17</sub>N<sub>3</sub>O<sub>4</sub>: C, 62.38%; H, 5.23%; N, 12.84%. Found: C, 62.08%; H, 5.05%; N, 12.75%.

**7-Methoxy-1-(((1S,2S,5R,6S)-6-methyl-4-oxo-3-azabicyclo[3.1.0]-hexan-2-yl)methoxy)-isoquinoline-6-carboxamide (45).** This was prepared from **17** and (*1R,4S,5S,6S*)-4-(hydroxymethyl)-6-methyl-3-azabicyclo[3.1.0]hexan-2-one (**43b**) according to the general procedure for the preparation of **40**; mp 238–240 °C. <sup>1</sup>H NMR (500 MHz, DMSO-*d*<sub>6</sub>) δ 8.17 (s, 1H), 7.90 (d, *J* = 5.6 Hz, 1H), 7.84 (br s, 1H), 7.70 (br s, 1H), 7.62 (s, 1H), 7.42 (d, *J* = 5.9 Hz, 1H), 4.45 (dd, *J* = 3.9, 10.8 Hz, 1H), 4.35 (dd, *J* = 5.6, 10.8 Hz, 1H), 4.00 (s, 3H), 3.89 (t, *J* = 4.5 Hz, 1H), 1.76–1.73 (m, 1H), 1.60–1.56 (m, 1H), 1.08 (d, *J* = 6.1 Hz, 3H), 1.02–0.97 (m, 1H). <sup>13</sup>C NMR (126 MHz, DMSO-*d*<sub>6</sub>) δ 176.78, 166.83, 159.05, 155.69, 138.29, 132.28, 130.75, 129.04, 120.80, 115.68, 103.28, 69.52, 56.49, 54.16, 27.20, 24.89, 19.78, 16.68. LCMS: 342 (MH<sup>+</sup>). HRMS: calcd mass for C<sub>18</sub>H<sub>20</sub>N<sub>3</sub>O<sub>4</sub> (MH<sup>+</sup>) 342.1448; found 342.1451; difference 0.9 ppm. HPLC purity: 95.77%.

**(3R,7aS)-6-Fluoro-3-(4-methoxyphenyl)-1,7a-dihydro-3H,5H-pyrrolo[1,2-c]oxazol-5-one (47).** To a solution of (*3R,7aS*)-3-(4-methoxyphenyl)tetrahydropyrrolo[1,2-c]oxazol-5(3H)-one (**46**, 16.0 g, 68.59 mmol) in THF (160 mL) was cooled to –78 °C and treated with LDA (2 M, 48 mL). After 30 min, a solution of NFSI (22.68 g, 72 mmol) in THF (80 mL) was added at –78 °C. After 30 min at –78 °C, the mixture was allowed to warm to 25 °C for 30 min. EtOAc and water were added, and the phases were separated. The aqueous phase was extracted with EtOAc, and the combined EtOAc extracts were washed with brine, dried over Na<sub>2</sub>SO<sub>4</sub>, filtered, and concentrated. The residue was purified

by chromatography to provide 12.4 g (72%) of (*3R,7aS*)-6-fluoro-3-(4-methoxyphenyl)tetrahydro-3*H*-pyrrolo[1,2-*c*]oxazol-5-one as a colorless oil. <sup>1</sup>H NMR (400 MHz, CDCl<sub>3</sub>) δ 7.36 (d, 2 H), 6.88 (d, 2 H), 6.22 (s, 1 H), 5.14 (dd, 1 H), 4.40–4.29 (m, 2 H), 3.79 (s, 1 H), 3.46 (dd, 1 H), 2.62–2.51 (m, 1 H), 2.23–2.07 (m, 1 H). The above intermediate (12.4 g, 49 mmol) was dissolved in THF (130 mL), cooled to –78 °C, and treated with LDA (2 M, 35 mL). After 30 min, a solution of diphenyl diselenide (16.96 g, 54 mmol) in THF (70 mL) was added at –78 °C. After 30 min at –78 °C, the mixture was allowed to warm to 25 °C for 30 min. EtOAc and water were added and the phases separated. The aqueous phase was extracted with EtOAc. The combined EtOAc extracts were washed with brine, dried over Na<sub>2</sub>SO<sub>4</sub>, filtered, and concentrated. The residue was purified by chromatography to provide 13 g (65%) of (*3R,7aS*)-6-fluoro-3-(4-methoxyphenyl)-6-(phenylselanyl)tetrahydropyrrolo-[1,2-*c*]oxazol-5(*H*)-one as a dark-yellow gum. This was used in the next step without further characterization. A solution of the selenide (13.0 g, 32 mmol) in DCM (260 mL) and pyridine (5.7 mL, 70 mmol) was treated with hydrogen peroxide (30%, 11.9 mL, 106 mmol) at 0 °C. The mixture was kept at 0 °C for 30 min, then allowed to warm to 25 °C for 2 h before being diluted with DCM and water. The DCM was separated, and the aqueous phase was extracted with DCM. The combined DCM extracts were washed with water and brine, dried over Na<sub>2</sub>SO<sub>4</sub>, filtered, and concentrated. The residue was purified by chromatography to provide 4.6 g (58%) of **47** as an off-white solid. <sup>1</sup>H NMR (400 MHz, CDCl<sub>3</sub>) δ 7.45 (d, *J* = 8.8 Hz, 2 H), 6.93 (d, *J* = 8.8 Hz, 2 H), 6.54 (t, *J* = 1.7 Hz, 1 H), 6.10 (s, 1 H), 4.55–4.47 (m, 1 H), 4.41–4.34 (m, 1 H), 3.83 (s, 3 H), 3.38 (t, *J* = 8.6 Hz, 1 H). <sup>19</sup>F NMR (376 MHz, CD<sub>3</sub>CN) δ –137.11. LCMS: 250 (MH<sup>+</sup>). HPLC purity: 98.63%.

**(3*R,5aS,6S,6aR,6bS*)-5*a*-Fluoro-3-(4-methoxyphenyl)-6-methyltetrahydro-1*H*-cyclopropa[3,4]pyrrolo-[1,2-*c*]oxazol-5(*H*)-one (48).** To a stirred suspension of ethyldiphenylsulfonium tetrafluoroborate (5.31 g, 17 mmol) in DME (62 mL) was added LDA (2 M, 8.0 mL) slowly with cooling to –55 °C (internal temperature). The reaction mixture was kept at –55 °C for 45 min, at which point, it was warmed to –35 °C and a solution of **47** (1.99 g, 8.0 mmol) in DME (20 mL) was added. The reaction mixture was maintained at –30 °C for 1.5 h, then aqueous NaHCO<sub>3</sub> and EtOAc were added. The EtOAc was separated, and the aqueous phase was extracted with EtOAc. The combined EtOAc extracts were dried over MgSO<sub>4</sub>, filtered, and concentrated. The residue was purified by chromatography to provide 362 mg (16%) of **48** as a white solid. <sup>1</sup>H NMR (400 MHz, CD<sub>3</sub>CN) δ 7.28 (d, *J* = 8.59 Hz, 2 H), 6.90 (d, *J* = 8.98 Hz, 2 H), 6.12 (s, 1 H), 4.17 (dd, *J* = 8.20, 5.85 Hz, 1 H), 3.78 (s, 3 H), 3.66–3.75 (m, 1 H), 3.45 (dd, *J* = 9.56, 8.39 Hz, 1 H), 2.33 (dd, *J* = 11.12, 4.10 Hz, 1 H), 1.64 (d, *J* = 0.78 Hz, 1 H), 1.25 (dd, *J* = 6.24, 1.56 Hz, 3 H). LCMS: 278 (MH<sup>+</sup>).

**(1*S,4S,5R,6S*)-1-Fluoro-4-(hydroxymethyl)-6-methyl-3-azabicyclo[3.1.0]hexan-2-one (49).** This compound was prepared from **48** according to the general procedure for the preparation of **35e**. <sup>1</sup>H NMR (400 MHz, CDCl<sub>3</sub>) δ 6.07 (br s, 1 H), 3.66–3.81 (m, 1 H), 3.54–3.67 (m, 1 H), 3.36–3.50 (m, 1 H), 1.77–1.87 (m, 2 H), 1.29 (d, *J* = 1.56 Hz, 3 H).

**1-((1*R,2S,5S,6S*)-5-Fluoro-6-methyl-4-oxo-3-azabicyclo[3.1.0]hexan-2-yl)methoxy)-7-methoxy-isoquinoline-6-carboxamide (50).** This was prepared from **17** and (*1S,4S,5R,6S*)-1-fluoro-4-(hydroxymethyl)-6-methyl-3-azabicyclo[3.1.0]hexan-2-one (**49**) according to the general procedure for the preparation of **40**; mp 275–278 °C. <sup>1</sup>H NMR (500 MHz, DMSO-*d*<sub>6</sub>) δ 8.17 (s, 1 H), 8.00 (br s, 1 H), 7.90 (d, *J* = 5.6 Hz, 1 H), 7.84 (br s, 1 H), 7.70 (br s, 1 H), 7.59 (s, 1 H), 7.43 (d, *J* = 5.9 Hz, 1 H), 4.52 (dd, *J* = 2.8, 11.1 Hz, 1 H), 4.38 (dd, *J* = 3.9, 11.0 Hz, 1 H), 3.96 (s, 3 H), 3.78–3.72 (m, 1 H), 2.21 (dd, *J* = 1.6, 10.4 Hz, 1 H), 1.32–1.25 (m, 1 H), 1.22 (d, *J* = 5.9 Hz, 3 H). <sup>13</sup>C NMR (126 MHz, DMSO-*d*<sub>6</sub>) δ 171.44 (d, *J* = 22.7 Hz, 1 C), 166.82, 158.92, 155.70, 138.29, 132.27, 130.83, 129.04, 120.76, 115.76, 103.05, 83.16 (d, *J* = 250.8 Hz, 1 C), 68.18, 56.36 (d, *J* = 2.5 Hz, 1 C), 52.89, 27.78 (d, *J* = 5.0 Hz, 1 C), 22.37 (d, *J* = 11.8 Hz, 1 C), 11.29 (d, *J* = 5.9 Hz, 1 C). <sup>19</sup>F NMR (H decoupled, 376 MHz, DMSO-*d*<sub>6</sub>) δ –223.39. LCMS: 360 (MH<sup>+</sup>). HRMS: calcd mass for C<sub>18</sub>H<sub>19</sub>FN<sub>3</sub>O<sub>4</sub> (MH<sup>+</sup>) 360.1354; found 360.136; difference 1.76 ppm. HPLC purity: 98.45%.

**2-Isopropoxybenzamide (51).** This compound was a commercially available sample in the Pfizer sample collection prior to the initiation of this project; mp 64–66 °C (literature mp 67–68 °C). <sup>58</sup> <sup>1</sup>H NMR (400 MHz, DMSO-*d*<sub>6</sub>) δ 7.84 (dd, *J* = 1.6, 7.8 Hz, 1 H), 7.57 (br s, 1 H), 7.52 (br s, 1 H), 7.48–7.40 (m, 1 H), 7.14 (d, *J* = 8.2 Hz, 1 H), 7.00 (t, *J* = 7.4 Hz, 1 H), 4.77 (spt, *J* = 6.0 Hz, 1 H), 1.33 (d, *J* = 5.9 Hz, 6 H). <sup>13</sup>C NMR (101 MHz, DMSO-*d*<sub>6</sub>) δ 166.28, 155.46, 132.36, 130.99, 123.36, 120.37, 114.45, 71.07, 21.70. LCMS: 180 (MH<sup>+</sup>). HPLC purity: 85.00%.

**Biological Assays. IRAK4 Enzymatic Assays. IRAK4 CALIPER Assay.** For the fragment screen, an IRAK4 Caliper assay was performed as follows. Purified human IRAK4 (Ren 64-1-N-6xHis full length) was diluted to a concentration 50 nM in assay buffer (20 mM HEPES pH 7.5, 10 mM MgCl<sub>2</sub>, 0.0005% Tween 20, 0.01% BSA, and 1 mM DTT) containing IRAK4 inhibitor (at 2× the final concentration) in 0.4% DMSO. The enzyme and inhibitor were allowed to incubate for 120 min at room temperature (25–27 °C). The reaction was started by the addition of an equal volume of the assay buffer containing 2 μM peptide (5-FAM-LPTSPITTYFFFKKK-COOH) and 700 μM ATP to achieve a final concentration of 25 nM enzyme, 1 μM peptide, 350 μM ATP, 1× compound, and 0.2% DMSO. The kinase reaction was allowed to run for 120 min at room temperature (25–27 °C). The reaction was stopped by the addition of EDTA to a final concentration of 10 mM. The extent of reaction was analyzed using the Caliper Lab Chip 3000 (PerkinElmer).

**IRAK4 DELFIA Assay.** For routine screening, an IRAK4 DELFIA (Dissociation-Enhanced Lanthanide Fluorescent Immunoassay, PerkinElmer) was performed. Purified human full length IRAK4 (Ren 64-1-N-6xHis) was diluted to 0.2 nM in assay buffer (20 mM HEPES pH 7.5, 5 mM MgCl<sub>2</sub>, 0.0025% Brij-35, and 1 mM DTT) containing IRAK4 inhibitor at 2× the final concentration in 5% DMSO. The enzyme and inhibitor were allowed to incubate for 20 min at room temperature. The reaction was started by the addition of an equal volume of the assay buffer containing 100 nM peptide substrate (biotinylated-AGAGRDKYKTLRQIR, ERM-peptide, AnaSpec) and 1.2 mM ATP to achieve a final concentration of 0.1 nM IRAK4 enzyme, 50 nM ERM-peptide, 600 μM ATP, 1× compound, and 2.5% DMSO. The kinase reaction was allowed to proceed for 60 min at room temperature and stopped by the addition of EDTA at a final concentration of 100 mM. Then, 50 μL of the stopped reaction mixture was transferred to a streptavidin coated DELFIA detection plate (PerkinElmer) and incubated for 30 min at room temperature while shaking at 700 rpm on a microplate shaker (VWR). The plate was washed 4 times with buffer (1× PBS containing 0.05% Tween-20) and then incubated with 50 μL of antibody cocktail consisting of Antiphospho-ERM at 0.125 μg/mL (Cell Signaling Technology) and Anti-Rabbit IgG EuN1 at 0.25 μg/mL (PerkinElmer) in a solution of 10 mM MOPS pH = 7.5, 150 mM NaCl, 0.05% Tween-20, 0.02% Na<sub>3</sub>N, 1% BSA, and 0.1% gelatin for 45 min while shaking and then washed as before. Next, 50 μL of DELFIA Enhancement Solution (PerkinElmer) was added to the plate and incubated for an additional 30 min at room temperature prior to being read on an EnVision model 2104 multilabel reader (PerkinElmer) using a 340 nm excitation wavelength and a 615 nm emission wavelength for detection.

**Cellular Assays. R848-Induced TNFa in Human PBMC Assay.** Human peripheral blood mononuclear cells (PBMCs) were purified from fresh human whole blood collected from healthy donors in heparin sulfate vacutainer tubes under informed consent and in compliance with institutional guidelines. Fresh blood (30 mL) was added to an ACCUSPIN tube (Sigma-Aldrich) containing 15 mL of Histopaque-1077 and centrifuged for 20 min at 1200g at room temperature with no brake. The interface layer of cells between the plasma and histopaque-1077, enriched with PBMCs, was collected and washed with 1× phosphate-buffered saline (PBS) several times until the supernatant was clear. The final PBMC pellet was resuspended in RPMI (Lonza) to a final concentration of 2 × 10<sup>6</sup> cells/mL. Then 50 μL of diluted PBMCs with 0.94 μg/mL R848 (Invivogen) were added to black-walled, tissue-culture treated 384-well plates containing 0.25 μL of test compound in DMSO at 200× to achieve a final concentration of DMSO equal to 0.5% and 1 × 10<sup>5</sup> PBMCs/well. Plates were covered with lids and incubated for 3 h at 37 °C in a humidified tissue-culture incubator. After a brief centrifugation (100g for 5 min), 15 μL of the supernatant was removed

for cytokine analysis on human TNF $\alpha$  ultrasensitive plates (Mesoscale Discovery).

**R848-Induced IL-6 in Human Whole Blood Assay.** Blood was collected from healthy male donors in heparin sulfate vacutainer tubes under informed consent and in compliance with institutional guidelines. Blood (200  $\mu$ L) was pipetted into 96-well polypropylene plates containing 2  $\mu$ L of test compound diluted in DMSO at 100 $\times$  final test concentration (final concentration of DMSO in assay is 1%). Blood was mixed for 45 s in the wells using a 96-well pin-tool (Scinomix). Plates were sealed with aluminum tape, and test compounds were preincubated with blood for 30 min prior to addition of 10  $\mu$ L of 5  $\mu$ g/mL R848 reconstituted in H<sub>2</sub>O (final R848 concentration in assay is 0.25  $\mu$ g/mL). Blood was mixed again for 45 s using a 96-well pin-tool. The plate was sealed with aluminum tape and incubated for 4 h at 37 °C without agitation. Plates were spun at 1500 rpm for 10 min, and 25  $\mu$ L of plasma was removed for cytokine analysis on human IL-6 ultrasensitive plates (Mesoscale Discovery).

**Rat LPS Model.** Rats (Sprague–Dawley male, 6–8 weeks of age, Charles River Laboratories, Wilmington, MA,  $n = 6$ –9 per treatment group) were orally dosed with the test article as a solution or suspension in the vehicle or vehicle alone (0.5% methylcellulose, 2% Tween 80 in water) 1 h before challenge of LPS (Invivogen Ultrapure, 0.01 mg/kg) intravenously. At 1.5 h post LPS challenge, blood was drawn for measurement of serum TNF by MSD. All procedures performed on these animals were in accordance with regulations and established guidelines and were reviewed and approved by the Pfizer Institutional Animal Care and Use Committee.

**Rat Collagen-Induced Arthritis (CIA) Model.<sup>59</sup>** Rats (Lewis female, approximately 7–9 weeks of age, Charles River Laboratories, Portage, MI,  $n = 10$  per treatment group) were immunized with an emulsion of type II collagen (CII, bovine) and incomplete Freund's adjuvant (IFA) on day 0 and received a boost of CII/IFA on day 7. Hind paw volume increase was taken by plethysmograph. Animals were randomly enrolled into treatment groups based on the development of disease. Beginning on day 11 post immunization, rats were enrolled into random treatment groups based on an increase in a single hind paw volume compared to day 7 post immunization baseline measurements. Day 0 was designated as the first treatment day. Animals were dosed orally, twice daily, with the test article (as a solution or suspension in the vehicle) or vehicle alone (0.5% methylcellulose, 2% Tween 80 in water). Paw measurements were taken daily by plethysmograph. The rats were weighed on a daily basis. At the end of the study, spleens were harvested, flash frozen, and assessed for kinase occupancy using an ATP-competitive probe in the KiNativ profiling assay<sup>60</sup> by ActivX Biosciences (La Jolla, CA). All procedures performed on these animals were in accordance with regulations and established guidelines and were reviewed and approved by the Pfizer Institutional Animal Care and Use Committee.

**Co-crystallization Methods. Purification of IRAK4 Protein for Co-crystallization.** Baculovirus cell paste containing the overexpressed recombinant IRAK4 catalytic domain (residues 154–460) protein was resuspended in 6 volumes of buffer A (50 mM Tris pH 7.8, 10% (v/v) glycerol, 250 mM NaCl, 1 mM TCEP, 10 mM imidazole, Complete EDTA-free protease inhibitor (1 tablet per 50 mL of buffer, Roche), and benzonase (1  $\mu$ L per 50 mL of buffer, Sigma). Cells were lysed with 1 pass on a microfluidizer (pressure at 18 K). The lysate was clarified by centrifugation at 4 °C for 30 min with a SS-34 rotor (Sorvall) at 12000 rpm.

The resultant supernatant was decanted and filtered through a VacuCap 90 PF bottle top filtration unit with a 0.8/0.2 Supor membrane (Pall). It was then direct-loaded using an Akta onto a HisTrap FF crude prepacked column (GE Healthcare) that was pre-equilibrated with buffer A. The column was washed with buffer A until a steady baseline was achieved. Protein was step eluted with 100% buffer B (50 mM Tris pH 7.8, 10% (v/v) glycerol, 250 mM NaCl, 1 mM TCEP, and 500 mM imidazole). Eluted fractions were pooled and treated with a 1:100 ratio of TEV protease (Accelagen) at 4 °C overnight to cleave the tag. Simultaneously, the protein was dialyzed into buffer C (50 mM Tris pH 7.8, 10% (v/v) glycerol, 20 mM NaCl, and 1 mM TCEP). The extent of tag cleavage was monitored by electrospray mass spectrometry. When the cleavage was complete, the protein was loaded onto a Q FF

prepacked column (GE Healthcare) that had been pre-equilibrated in buffer C. The column was washed with buffer C until a steady baseline was achieved. The protein was eluted with a 0–100% gradient of buffer D (50 mM Tris pH 7.8, 10% (v/v) glycerol, 1000 mM NaCl, and 1 mM TCEP) at 10 mM NaCl per column volume. The eluted fractions were combined, and the protein was concentrated to a volume of 5 mL using an Amicon Ultrafree-15 centrifugal filtration device with a molecular weight cutoff of 10K (Millipore). The sample was loaded onto a HiPrep 16/60 Superdex 75 column that had been pre-equilibrated in buffer E (50 mM Tris pH 7.6, 10% (v/v) glycerol, 250 mM NaCl, and 1 mM TCEP). The peak fractions were collected and concentrated to 12 mg/mL. They were then aliquoted and flash frozen in liquid nitrogen for storage.

**Crystallization.** The protein was incubated with 2 mM compound (2% DMSO) for 30 min prior to setting up trays. Plate crystals were grown over several days at 22 °C using the hanging drop vapor diffusion method. Then 1 + 1  $\mu$ L drops were set over 500  $\mu$ L of well solution in VDXm plates (Hampton Research). The well solution consisted of 1.6–1.8 M ammonium citrate pH 7.0.

**Structure Determination.** The crystals were cryoprotected in a solution of mother liquor plus 20% glycerol. They were then flash frozen in liquid nitrogen for data collection at the Advanced Photon Source, Beamline 17 (Argonne, IL).

**Nuclear Magnetic Resonance (NMR).** For the fragment screen, IRAK4 catalytic domain (residues 154–460) was screened against a proprietary 2592 member fragment library, referred to as GFI-1<sup>46</sup> using 1D saturation transfer difference<sup>61</sup> (STD) spectroscopy in NMR. A 3  $\mu$ M protein solution was prepared in 25 mM Hepes-*d*<sub>18</sub> (Cambridge Isotope Laboratories, DLM-1814), 200 mM NaCl, 1 mM TCEP in 75% D<sub>2</sub>O (Cambridge Isotope Laboratories, DLM-499), pH 7.5. Fragments were preloaded in mixtures of 10 at 10 mM each in DMSO-*d*<sub>6</sub> or in mixtures of 4 at 50 mM each in DMSO-*d*<sub>6</sub>. Protein solution at 3  $\mu$ M was added to the fragment mixtures for a final fragment concentration equal to 230  $\mu$ M each. The 1D STD NMR experiment was carried out using a Varian Inova 600 MHz NMR spectrometer equipped with 100 position sample robotics system (Zymark). In the STD experiment, a 2.0 s sinc-shaped pulse was applied for on resonance saturation –2700 Hz from the carrier and applied for off-resonance saturation –102700 Hz from the carrier. Positive signals in the difference spectra indicate ligand binding, and the identification of the bound ligand in the mixture was determined by comparison to 1D <sup>1</sup>H reference NMR spectra of each fragment. Data were analyzed using an internal software package.

**Molecular Modeling Methods.** WaterMap calculations were run using WaterMap (Schrodinger, version 2012) with the ligand in the active site. A 2 ns trajectory was utilized. The initial pose was generated using Protein Preparation Wizard (Schrodinger, version 2012) with the crystallographic waters removed. The OPLS\_2005 force field was used for all calculations.

## ASSOCIATED CONTENT

### S Supporting Information

The Supporting Information is available free of charge on the ACS Publications website at DOI: [10.1021/acs.jmedchem.7b00231](https://doi.org/10.1021/acs.jmedchem.7b00231).

<sup>1</sup>H and <sup>13</sup>C NMR spectra of compounds **10**, **12**, **14**, **16**, **21**–**24**, **26**, **30**–**33**, **36**–**41**, **44**, **45**, **50**, **51**; X-ray structures of **34e**, **42b**, **48**; selectivity of compounds **20** and **40** in kinase panels ([PDF](#))  
Molecular formula strings ([CSV](#))

### Accession Codes

Crystal structure of IRAK4 in complex with compounds **51** PDBSUIQ, **12** PDB SUIR, **14** PDB SUIS, **20** PDB SUIT, **40** PDB SUIU.

## AUTHOR INFORMATION

### Corresponding Authors

\*For K.L.L.: phone, 617-674-7299; E-mail, [katherine.lee@pfizer.com](mailto:katherine.lee@pfizer.com).

\*For S.W.W.: phone, 860-441-5831; E-mail, [stephen.w.wright@pfizer.com](mailto:stephen.w.wright@pfizer.com).

### ORCID

Katherine L. Lee: [0000-0003-0155-290X](http://orcid.org/0000-0003-0155-290X)

Frank E. Lovering: [0000-0002-9515-8200](http://orcid.org/0000-0002-9515-8200)

### Present Addresses

<sup>†</sup>David R. Anderson, Luc Therapeutics, Inc., 400 Technology Square, Cambridge, Massachusetts 02139, United States.

<sup>+\*</sup>Seungwon Chung, AbbVie, 1 North Waukegan Road, North Chicago, Illinois 60064–6123, United States.

● Kevin J. Curran, Chromocell Corporation, 685 US Highway One, North Brunswick, New Jersey 08902, United States.

◇ Jacqueline E. Day, MilliporeSigma, 2909 Lacledes Avenue, Saint Louis, Missouri 63103, United States.

□ Christoph M. Dehnhardt, Xenon Pharmaceuticals, 3650 Gilmore Way, Burnaby, British Columbia V5G 4W8, Canada.

▲ Lori K. Gavrin, GSK, 1250 Collegeville Road, Collegeville, Pennsylvania 19085, United States.

<sup>②</sup>Joel A. Goldberg, University Hospitals Cleveland Medical Center, 11100 Euclid Avenue, Cleveland, Ohio 44106, United States.

■ Heidi R. Hope, Confluence Discovery Technologies, 4320 Forest Park Avenue, St. Louis, Missouri 63108, United States.

▼ Michael D. Lowe, Boehringer Ingelheim Pharmaceuticals, Inc., Ridgefield, Connecticut 06877, United States.

★ Heidi M. Morgan, ForteBio, a division of Pall Life Sciences, 1360 Willow Road, Suite 210, Menlo Park, California 94025, United States.

<sup>④</sup>Nikolaos Papaioannou, Shire, 125 Spring Street, Lexington, Massachusetts 02421, United States.

◊ Akshay Patny, EMD Serono Research & Development Institute, Inc., 45A Middlesex Turnpike, Billerica, Massachusetts 01821, United States.

◆ Betsy S. Pierce, Kalexsyn, Inc., 4502 Campus Drive, Kalamazoo, Michigan 49008, United States.

<sup>⑤</sup>Eddine Saiah, Navitor Pharmaceuticals, 1030 Massachusetts Avenue, Cambridge, Massachusetts 02446, United States.

○ Holly H. Soutter, X-Chem., Inc., 100 Beaver Street, Waltham, Massachusetts 02453, United States.

♦ John D. Trzupek, KSQ Therapeutics, 790 Memorial Drive, Suite 200, Cambridge, Massachusetts 02139, United States.

<sup>⑥</sup>Jennifer R. Thomason, Forma Therapeutics, Inc., 500 Arsenal Street, Suite 100, Watertown, Massachusetts 02472 United States.

► Richard Vargas, Amgen, 360 Binney Street, Cambridge, Massachusetts 02142, United States.

◀ Christoph W. Zapf, Nurix, Inc., 1700 Owens Street, Suite 205, San Francisco, California 94158, United States.

### Author Contributions

K.L.L., S.W.W., F.E.L., D.R.A., B.S.P., J.D.T., L.K.G., A.L., E.S., M.D.L., K.J.C., C.M.D., J.A.G., J.R.T., R.V., J.W.S., N.P., C.W.Z., A.P., S.E.D., S.C., C.C., B.P.B., J.P.M., and D.H. performed medicinal chemistry; S.H., J.S.C., S.K., J.E.D., and H.H.S. conducted cocrystallization; Y.U. conducted NMR fragment screening; V.R.R., L.-L.L., H.R.H., and I.C.K. led biology efforts; M.W.H.S., H.M.M., E.A.M., J.H.S., R.K.F., F.V., and K.D. developed and/or performed in vitro assays; M.H., P.T.S., and A.G.B. performed in vivo studies; J.I.B. led pharmacokinetic

efforts; C.M.A. provided formulation expertise; and B.M.S. and I.J.S. performed small molecule crystallization.

### Notes

The authors declare no competing financial interest.

## ACKNOWLEDGMENTS

We thank Jeffrey Culp and Pat Loulakis for IRAK4 protein production; Kimberly Lapham and Wei Song for assistance with pharmacokinetic studies; Ann Wrightstone, Simeon Ramsey, Aaron Winkler, Margaret Fleming, Ju Wang, Bruce Jacobsen, and Paul Morgan for assistance with biology assays; Ravi Garigipati, Bryan Li, Stephen Kortum, Christophe Allais, Alpay Dermenci, Jit Basak, and Jotham Coe for synthesis support; John Davis for support for safety studies; and Jane Withka and Ravi Kurumbail for assistance with fragment screening data.

## ABBREVIATIONS USED

CIA, collagen induced arthritis; CL, clearance; FQ, fit quality; hERG, human ether-a-go-go-related gene; HLM, human liver microsomes; IRAK4, interleukin-1 receptor associated kinase 4; IL-1, interleukin-1; IV, intravenous; LE, ligand efficiency; LipE, lipophilic efficiency; LPS, lipopolysaccharide; MYD88, myeloid differentiation primary response gene 88;  $P_{app}$ , apparent permeability; PBMC, peripheral blood mononuclear cell; RA, rheumatoid arthritis; STD, saturation transfer difference; SLE, systemic lupus erythematosus; TLR, Toll-like receptor; Vss, steady-state volume of distribution

## REFERENCES

- (1) Maglione, P. J.; Simchoni, N.; Black, S.; Radigan, L.; Overbey, J. R.; Bagiella, E.; Bussel, J. B.; Bossuyt, X.; Casanova, J.-L.; Meyts, I.; Cerutti, A.; Picard, C.; Cunningham-Rundles, C. IRAK-4 and MyD88 deficiencies impair IgM responses against T-independent bacterial antigens. *Blood* **2014**, *124*, 3561–3571.
- (2) Suzuki, N.; Suzuki, S.; Millar, D. G.; Unno, M.; Hara, H.; Calzascia, T.; Yamasaki, S.; Yokosuka, T.; Chen, N.-J.; Elford, A. R.; Suzuki, J.-I.; Takeuchi, A.; Mirtsos, C.; Bouchard, D.; Ohashi, P. S.; Yeh, W.-C.; Saito, T. A critical role for the innate immune signaling molecule IRAK-4 in T cell activation. *Science* **2006**, *311*, 1927–1932.
- (3) Suzuki, N.; Chen, N. J.; Millar, D. G.; Suzuki, S.; Horacek, T.; Hara, H.; Bouchard, D.; Nakanishi, K.; Penninger, J. M.; Ohashi, P. S.; Yeh, W. C. IL-1 receptor-associated kinase 4 is essential for IL-18-mediated NK and Th1 cell responses. *J. Immunol.* **2003**, *170*, 4031–4035.
- (4) McDonald, D. R.; Goldman, F.; Gomez-Duarte, O. D.; Issekutz, A. C.; Kumararatne, D. S.; Doffinger, R.; Geha, R. S. Impaired T-cell receptor activation in IL-1 receptor-associated kinase-4-deficient patients. *J. Allergy Clin. Immunol.* **2010**, *126*, 332–337.
- (5) Suzuki, N.; Saito, T. IRAK-4—a shared NF-κB activator in innate and acquired immunity. *Trends Immunol.* **2006**, *27*, 566–572.
- (6) Cushing, L.; Stochaj, W.; Siegel, M.; Czerwinski, R.; Dower, K.; Wright, Q.; Hirschfield, M.; Casanova, J. L.; Picard, C.; Puel, A.; Lin, L. L.; Rao, V. R. Interleukin 1/Toll-like receptor-induced autophasphorylation activates interleukin 1 receptor-associated kinase 4 and controls cytokine induction in a cell type-specific manner. *J. Biol. Chem.* **2014**, *289*, 10865–10875.
- (7) Fraczek, J.; Kim, T. W.; Xiao, H.; Yao, J.; Wen, Q.; Li, Y.; Casanova, J. L.; Pryjma, J.; Li, X. The kinase activity of IL-1 receptor-associated kinase 4 is required for interleukin-1 receptor/toll-like receptor-induced TAK1-dependent NFκB activation. *J. Biol. Chem.* **2008**, *283*, 31697–31705.
- (8) Ku, C. L.; von Bernuth, H.; Picard, C.; Zhang, S. Y.; Chang, H. H.; Yang, K.; Chrabieh, M.; Issekutz, A. C.; Cunningham, C. K.; Gallin, J.; Holland, S. M.; Roifman, C.; Ehl, S.; Smart, J.; Tang, M.; Barrat, F. J.; Levy, O.; McDonald, D.; Day-Good, N. K.; Miller, R.; Takada, H.; Hara, T.; Al-Hajjar, S.; Al-Ghonaime, A.; Speert, D.; Sanlaville, D.; Li, X.; Geissmann, F.; Vivier, E.; Marodi, L.; Garty, B. Z.; Chapel, H.;

- Rodriguez-Gallego, C.; Bossuyt, X.; Abel, L.; Puel, A.; Casanova, J. L. Selective predisposition to bacterial infections in IRAK-4-deficient children: IRAK-4-dependent TLRs are otherwise redundant in protective immunity. *J. Exp. Med.* **2007**, *204*, 2407–2422.
- (9) Yang, K.; Puel, A.; Zhang, S.; Eidenschenk, C.; Ku, C. L.; Casrouge, A.; Picard, C.; von Bernuth, H.; Senechal, B.; Plancoulaine, S.; Al-Hajjar, S.; Al-Ghonioun, A.; Marodi, L.; Davidson, D.; Speert, D.; Roifman, C.; Garty, B. Z.; Ozinsky, A.; Barrat, F. J.; Coffman, R. L.; Miller, R. L.; Li, X.; Lebon, P.; Rodriguez-Gallego, C.; Chapel, H.; Geissmann, F.; Jouanguy, E.; Casanova, J. L. Human TLR-7, -8, and -9-mediated induction of IFN-alpha/beta and -lambda is IRAK-4 dependent and redundant for protective immunity to viruses. *Immunity* **2005**, *23*, 465–478.
- (10) Sokolove, J.; Zhao, X.; Chandra, P. E.; Robinson, W. H. Immune complexes containing citrullinated fibrinogen costimulate macrophages via Toll-like receptor 4 and Fc gamma receptor. *Arthritis Rheum.* **2011**, *63*, 53–62.
- (11) Kono, D. H.; Haraldsson, M. K.; Lawson, B. R.; Pollard, K. M.; Koh, Y. T.; Du, X.; Arnold, C. N.; Baccala, R.; Silverman, G. J.; Beutler, B. A.; Theofilopoulos, A. N. Endosomal TLR signaling is required for anti-nucleic acid and rheumatoid factor autoantibodies in lupus. *Proc. Natl. Acad. Sci. U. S. A.* **2009**, *106*, 12061–12066.
- (12) Green, N. M.; Marshak-Rothstein, A. Toll-like receptor driven B cell activation in the induction of systemic autoimmunity. *Semin. Immunol.* **2011**, *23*, 106–112.
- (13) Kim, T. W.; Staschke, K.; Bulek, K.; Yao, J.; Peters, K.; Oh, K. H.; Vandenburg, Y.; Xiao, H.; Qian, W.; Hamilton, T.; Min, B.; Sen, G.; Gilmour, R.; Li, X. A critical role for IRAK4 kinase activity in Toll-like receptor-mediated innate immunity. *J. Exp. Med.* **2007**, *204*, 1025–1036.
- (14) Koziczak-Holbro, M.; Littlewood-Evans, A.; Pollinger, B.; Kovarik, J.; Dawson, J.; Zenke, G.; Burkhardt, C.; Muller, M.; Gram, H. The critical role of kinase activity of interleukin-1 receptor-associated kinase 4 in animal models of joint inflammation. *Arthritis Rheum.* **2009**, *60*, 1661–1671.
- (15) Rekhter, M.; Staschke, K.; Estridge, T.; Rutherford, P.; Jackson, N.; Gifford-Moore, D.; Foxworthy, P.; Reidy, C.; Huang, X.-d.; Kalbfleisch, M.; Hui, K.; Kuo, M.-S.; Gilmour, R.; Vlahos, C. J. Genetic ablation of IRAK4 kinase activity inhibits vascular lesion formation. *Biochem. Biophys. Res. Commun.* **2008**, *367*, 642–648.
- (16) Staschke, K. A.; Dong, S.; Saha, J.; Zhao, J.; Brooks, N. A.; Hepburn, D. L.; Xia, J.; Gulen, M. F.; Kang, Z.; Altuntas, C. Z.; Tuohy, V. K.; Gilmour, R.; Li, X.; Na, S. IRAK4 kinase activity is required for Th17 differentiation and Th17-mediated disease. *J. Immunol.* **2009**, *183*, 568–577.
- (17) Cameron, B.; Tse, W.; Lamb, R.; Li, X.; Lamb, B. T.; Landreth, G. E. Loss of interleukin receptor-associated kinase 4 signaling suppresses amyloid pathology and alters microglial phenotype in a mouse model of Alzheimer's disease. *J. Neurosci.* **2012**, *32*, 15112–15123.
- (18) Tumey, L. N.; Boschelli, D. H.; Bhagirath, N.; Shim, J.; Murphy, E. A.; Goodwin, D.; Bennett, E. M.; Wang, M.; Lin, L.-L.; Press, B.; Shen, M.; Frisbie, R. K.; Morgan, P.; Mohan, S.; Shin, J.; Rao, V. R. Identification and optimization of indolo[2,3-c]quinoline inhibitors of IRAK4. *Bioorg. Med. Chem. Lett.* **2014**, *24*, 2066–2072.
- (19) Kelly, P. N.; Romero, D. L.; Yang, Y.; Shaffer, A. L., III; Chaudhary, D.; Robinson, S.; Miao, W.; Rui, L.; Westlin, W. F.; Kapeller, R.; Staudt, L. M. Selective interleukin-1 receptor-associated kinase 4 inhibitors for the treatment of autoimmune disorders and lymphoid malignancy. *J. Exp. Med.* **2015**, *212*, 2189–2201.
- (20) Kondo, M.; Tahara, A.; Hayashi, K.; Abe, M.; Inami, H.; Ishikawa, T.; Ito, H.; Tomura, Y. Renoprotective effects of novel interleukin-1 receptor-associated kinase 4 inhibitor AS2444697 through anti-inflammatory action in 5/6 nephrectomized rats. *Naunyn-Schmiedeberg's Arch. Pharmacol.* **2014**, *387*, 909–919.
- (21) Dudhgaonkar, S.; Ranade, S.; Nagar, J.; Subramani, S.; Prasad, D. S.; Karunanithi, P.; Srivastava, R.; Venkatesh, K.; Selvam, S.; Krishnamurthy, P.; Mariappan, T. T.; Saxena, A.; Fan, L.; Stetsko, D. K.; Holloway, D. A.; Li, X.; Zhu, J.; Yang, W.-P.; Ruepp, S.; Nair, S.; Santella, J.; Duncia, J.; Hynes, J.; McIntyre, K. W.; Carman, J. A. Selective IRAK4 inhibition attenuates disease in murine lupus models and demonstrates steroid sparing activity. *J. Immunol.* **2017**, *198*, 1308–1319.
- (22) Wang, Z.; Liu, J.; Sudom, A.; Ayres, M.; Li, S.; Wesche, H.; Powers, J. P.; Walker, N. P. C. Crystal structures of IRAK-4 kinase in complex with inhibitors: A serine/threonine kinase with tyrosine as a gatekeeper. *Structure (Oxford, U. K.)* **2006**, *14*, 1835–1844.
- (23) Powers, J. P.; Li, S.; Jaen, J. C.; Liu, J.; Walker, N. P. C.; Wang, Z.; Wesche, H. Discovery and initial SAR of inhibitors of interleukin-1 receptor-associated kinase-4. *Bioorg. Med. Chem. Lett.* **2006**, *16*, 2842–2845.
- (24) Wang, Z.; Sun, D.; Johnstone, S.; Cao, Z.; Gao, X.; Jaen, J. C.; Liu, J.; Lively, S.; Miao, S.; Sudom, A.; Tomooka, C.; Walker, N. P. C.; Wright, M.; Yan, X.; Ye, Q.; Powers, J. P. Discovery of potent, selective, and orally bioavailable inhibitors of interleukin-1 receptor-associated kinase-4. *Bioorg. Med. Chem. Lett.* **2015**, *25*, 5546–5550.
- (25) Buckley, G. M.; Ceska, T. A.; Fraser, J. L.; Gowers, L.; Groom, C. R.; Higuero, A. P.; Jenkins, K.; Mack, S. R.; Morgan, T.; Parry, D. M.; Pitt, W. R.; Rausch, O.; Richard, M. D.; Sabin, V. IRAK-4 inhibitors. Part II: A structure-based assessment of imidazo[1,2-a]pyridine binding. *Bioorg. Med. Chem. Lett.* **2008**, *18*, 3291–3295.
- (26) Buckley, G. M.; Fosbeary, R.; Fraser, J. L.; Gowers, L.; Higuero, A. P.; James, L. A.; Jenkins, K.; Mack, S. R.; Morgan, T.; Parry, D. M.; Pitt, W. R.; Rausch, O.; Richard, M. D.; Sabin, V. IRAK-4 inhibitors. Part III: A series of imidazo[1,2-a]pyridines. *Bioorg. Med. Chem. Lett.* **2008**, *18*, 3656–3660.
- (27) McElroy, W. T.; Michael Seganish, W.; Jason Herr, R.; Harding, J.; Yang, J.; Yet, L.; Komanduri, V.; Prakash, K. C.; Lavey, B.; Tulshian, D.; Greenlee, W. J.; Sondey, C.; Fischmann, T. O.; Niu, X. Discovery and hit-to-lead optimization of 2,6-diaminopyrimidine inhibitors of interleukin-1 receptor-associated kinase 4. *Bioorg. Med. Chem. Lett.* **2015**, *25*, 1836–1841.
- (28) McElroy, W. T.; Tan, Z.; Ho, G.; Paliwal, S.; Li, G.; Seganish, W. M.; Tulshian, D.; Tata, J.; Fischmann, T. O.; Sondey, C.; Bian, H.; Bober, L.; Jackson, J.; Garlisi, C. G.; Devito, K.; Fossetta, J.; Lundell, D.; Niu, X. Potent and selective amidopyrazole inhibitors of IRAK4 that are efficacious in a rodent model of inflammation. *ACS Med. Chem. Lett.* **2015**, *6*, 677–682.
- (29) Lim, J.; Altman, M. D.; Baker, J.; Brubaker, J. D.; Chen, H.; Chen, Y.; Fischmann, T.; Gibeau, C.; Kleinschek, M. A.; Leccese, E.; Lesburg, C.; MacLean, J. K. F.; Moy, L. Y.; Mulrooney, E. F.; Presland, J.; Rakhilina, L.; Smith, G. F.; Steinhuebel, D.; Yang, R. Discovery of 5-amino-N-(1H-pyrazol-4-yl)pyrazolo[1,5-a]pyrimidine-3-carboxamide inhibitors of IRAK4. *ACS Med. Chem. Lett.* **2015**, *6*, 683–688.
- (30) Chaudhary, D.; Robinson, S.; Romero, D. L. Recent advances in the discovery of small molecule inhibitors of interleukin-1 receptor-associated kinase 4 (IRAK4) as a therapeutic target for inflammation and oncology disorders. *J. Med. Chem.* **2015**, *58*, 96–110.
- (31) Hynes, J., Jr.; Nair, S. K. Advances in the discovery of small-molecule IRAK4 inhibitors. *Annu. Rev. Med. Chem.* **2014**, *49*, 117–133.
- (32) Seganish, W. M. Inhibitors of interleukin-1 receptor-associated kinase 4 (IRAK4): a patent review (2012–2015). *Expert Opin. Ther. Pat.* **2016**, *26*, 917–932.
- (33) Wang, Z.; Wesche, H.; Stevens, T.; Walker, N.; Yeh, W.-C. IRAK-4 inhibitors for inflammation. *Curr. Top. Med. Chem.* **2009**, *9*, 724–737.
- (34) (a) Congreve, M.; Chessari, G.; Tisi, D.; Woodhead, A. J. Recent developments in fragment-based drug discovery. *J. Med. Chem.* **2008**, *51*, 3661–3680. (b) Erlanson, D. A.; Fesik, S. W.; Hubbard, R. E.; Jahnke, W.; Jhoti, H. Twenty years on: the impact of fragments on drug discovery. *Nat. Rev. Drug Discovery* **2016**, *15*, 605–619.
- (35) Ramsey, V. G.; Cretcher, L. H. Studies in the quinoline series; some 6-beta-hydroxyethoxy-4-aminoquinolines. *J. Am. Chem. Soc.* **1947**, *69*, 1659–62. (b) Robinson, R. A. 1-Dialkylaminoalkylaminoisoquinolines. *J. Am. Chem. Soc.* **1947**, *69*, 1939–1942.
- (36) Compounds **13** and **19** were prepared following the route described by Morgentin, R.; Pasquet, G.; Boutron, P.; Jung, F.; Lamorlette, M.; Maudet, M.; Ple, P. Strategic studies in the syntheses of novel 6,7-substituted quinolones and 7- or 6-substituted 1,6- and 1,7-naphthyridones. *Tetrahedron* **2008**, *64* (12), 2772–2782. Compounds **15**, **17**, and **18** were prepared following the routes described by

- (i) Kucznerz, R.; Dickhaut, J.; Leinert, H.; Von Der Saal, W. Improved procedures for large scale preparation of 6- and 7-oxy-substituted isoquinolines and a convenient work-up protocol for titanium supported reactions. *Synth. Commun.* **1999**, *29*, 1617–1625. (ii) Middleton, D. S.; Maw, G. N.; Challenger, C.; Jessiman, A.; Johnson, P. S.; Million, W. A.; Nichols, C. L.; Price, J. A.; Trevethick, M. Highly potent and selective zwitterionic agonists of the  $\delta$ -opioid receptor. Part I. *Bioorg. Med. Chem. Lett.* **2006**, *16*, 905–910. See also reference 35b.
- (37) Anderson, D. R.; Bunnage, M. E.; Curran, K. J.; Dehnhardt, C. M.; Gavrin, L. K.; Goldberg, J. A.; Han, S.; Hepworth, D.; Huang, H.-C.; Lee, A.; Lee, K. L.; Lovering, F. E.; Lowe, M. D.; Mathias, J. P.; Papaioannou, N.; Patny, A.; Pierce, B. S.; Saiah, E.; Strohbach, J. W.; Trzupek, J. D.; Vargas, R.; Wang, X.; Wright, S. W.; Zapf, C. W. Bicyclic-fused heteroaryl or aryl compounds as IRAK4 inhibitors and their preparation. WO2015150995A1, 2015.
- (38) Wright, S. W.; Choi, C.; Chung, S.; Boscoe, B. P.; Drozda, S. E.; Mousseau, J. J.; Trzupek, J. D. Reversal of diastereoselection in the conjugate addition of cuprates to unsaturated lactams. *Org. Lett.* **2015**, *17*, 5204–5207.
- (39) Konas, D. W.; Coward, J. K. Electrophilic fluorination of pyroglutamic acid derivatives: Application of substrate-dependent reactivity and diastereoselectivity to the synthesis of optically active 4-fluoroglutamic acids. *J. Org. Chem.* **2001**, *66*, 8831–8842.
- (40) Konas, D. W.; Coward, J. K. Synthesis of L-4,4-difluoroglutamic acid via electrophilic difluorination of a lactam. *Org. Lett.* **1999**, *1*, 2105–2107.
- (41) Davies, S. G.; Dixon, D. J.; Doisneau, G. J. M.; Prodger, J. C.; Sangane, H. J. Synthesis and utility of the 3,3-dimethyl-5-substituted-2-pyrrolidinone 'Quat' chiral auxiliary. *Tetrahedron: Asymmetry* **2002**, *13*, 647–658.
- (42) The diastereomer ratios were typically 2:1 to 3:1 in favor of the anti isomers.
- (43) Nagasaka, T.; Imai, T. Synthesis of chiral pyrrolidine derivatives from (S)-pyroglutamic acid. II. 4-(Hydroxymethyl)-3-azabicyclo[3.1.0]-hexan-2-ones and 5,5-disubstituted 2-pyrrolidinones. *Chem. Pharm. Bull.* **1997**, *45*, 36–42.
- (44) Zhang, R.; Mamai, A.; Madalenoitia, J. S. Cyclopropanation reactions of pyroglutamic acid-derived synthons with alkylidene transfer reagents. *J. Org. Chem.* **1999**, *64*, 547–555.
- (45) Nagasaka, T.; Imai, T. Synthesis of chiral pyrrolidine derivatives from (S)-pyroglutamic acid. I: 7-substituted (2R,SS)-2-aryl-1-aza-3-oxabicyclo[3.3.0]octan-8-ones, 7-substituted (2R,SS)-2-aryl-1-aza-3-oxabicyclo[3.3.0]oct-6-en-8-ones and 3-substituted (S)-5-(hydroxymethyl)-2-pyrrolidinones. *Chem. Pharm. Bull.* **1995**, *43*, 1081–8.
- (46) Lau, W. F.; Withka, J. M.; Hepworth, D.; Magee, T. V.; Du, Y. J.; Bakken, G. A.; Miller, M. D.; Hendsch, Z. S.; Thanabal, V.; Kolodziej, S. A.; Xing, L.; Hu, Q.; Narasimhan, L. S.; Love, R.; Charlton, M. E.; Hughes, S.; van Hoorn, W. P.; Mills, J. E. Design of a multi-purpose fragment screening library using molecular complexity and orthogonal diversity metrics. *J. Comput.-Aided Mol. Des.* **2011**, *25*, 621–636.
- (47) Leeson, P. D.; Springthorpe, B. The influence of drug-like concepts on decision-making in medicinal chemistry. *Nat. Rev. Drug Discovery* **2007**, *6*, 881–90.
- (48) Ryckmans, T.; Edwards, M. P.; Horne, V. A.; Correia, A. M.; Owen, D. R.; Thompson, L. R.; Tran, I.; Tutt, M. F.; Young, T. Rapid assessment of a novel series of selective CB(2) agonists using parallel synthesis protocols: A Lipophilic Efficiency (LipE) analysis. *Bioorg. Med. Chem. Lett.* **2009**, *19*, 4406–4409.
- (49) Lovering, F.; Bikker, J.; Humblet, C. Escape from flatland: Increasing saturation as an approach to improving clinical success. *J. Med. Chem.* **2009**, *52*, 6752–6756.
- (50) Di, L.; Whitney-Pickett, C.; Umland, J. P.; Zhang, H.; Zhang, X.; Gebhard, D. F.; Lai, Y.; Federico, J. J.; Davidson, R. E.; Smith, R.; Reyner, E. L.; Lee, C.; Feng, B.; Rotter, C.; Varma, M. V.; Kempshall, S.; Fenner, K.; El-kattan, A. F.; Liston, T. E.; Troutman, M. D. Development of a new permeability assay using low-efflux MDCKII cells. *J. Pharm. Sci.* **2011**, *100*, 4974–4985.
- (51) Zientek, M.; Miller, H.; Smith, D.; Dunklee, M. B.; Heinle, L.; Thurston, A.; Lee, C.; Hyland, R.; Fahmi, O.; Burdette, D. Development of an in vitro drug-drug interaction assay to simultaneously monitor five cytochrome P450 isoforms and performance assessment using drug library compounds. *J. Pharmacol. Toxicol. Methods* **2008**, *58*, 206–214.
- (52) Young, T.; Abel, R.; Kim, B.; Berne, B. J.; Friesner, R. A. Motifs for molecular recognition exploiting hydrophobic enclosure in protein-ligand binding. *Proc. Natl. Acad. Sci. U. S. A.* **2007**, *104*, 808–813.
- (53) Wang, L.; Berne, B. J.; Friesner, R. A. Ligand binding to protein-binding pockets with wet and dry regions. *Proc. Natl. Acad. Sci. U. S. A.* **2011**, *108*, 1326–1330.
- (54) Fernandez, A. Keeping dry and crossing membranes. *Nat. Biotechnol.* **2004**, *22*, 1081–1084.
- (55) Fraser, C. M.; Fernandez, A.; Scott, L. R. Dehydron analysis: quantifying the effect of hydrophobic groups on the strength and stability of hydrogen bonds. *Adv. Exp. Med. Biol.* **2010**, *680*, 473–479.
- (56) Compound 40 is commercially available via Sigma Aldrich (catalogue no. PZ0327).
- (57) Bavin, E. M.; Macrae, F. J.; Seymour, D. E.; Waterhouse, P. D. The analgesic and antipyretic properties of some derivatives of salicylamide. *J. Pharm. Pharmacol.* **1952**, *4*, 872–8.
- (58) Woodcock, D.; Davies, B. L. Synthesis of plant-growth regulators. V. (3-Substituted-2-naphthoxy)-n-alkanecarboxylic acids. *J. Chem. Soc.* **1958**, 4723–4728.
- (59) Hegen, M.; Keith, J. C., Jr.; Collins, M.; Nickerson-Nutter, C. L. Utility of animal models for identification of potential therapeutics for rheumatoid arthritis. *Ann. Rheum. Dis.* **2008**, *67*, 1505–1515.
- (60) Patricelli, M. P.; Nomanbhoy, T. K.; Wu, J.; Brown, H.; Zhou, D.; Zhang, J.; Jagannathan, S.; Aban, A.; Okerberg, E.; Herring, C.; Nordin, B.; Weissig, H.; Yang, Q.; Lee, J.-D.; Gray, N. S.; Kozarich, J. W. In situ kinase profiling reveals functionally relevant properties of native kinases. *Chem. Biol. (Oxford, U. K.)* **2011**, *18*, 699–710.
- (61) Mayer, M.; Meyer, B. Characterization of ligand binding by saturation transfer difference NMR spectroscopy. *Angew. Chem., Int. Ed.* **1999**, *38*, 1784–1788.